l'institut d'électronique

Thermophotovoltaics

Rodolphe Vaillon

Institut d'Electronique et des Systèmes, Univ Montpellier, CNRS, Montpellier, France

Note: the texts underlined in blue are internet links

May 12, 2022 version

Outline

Introduction
Basics of thermophotovoltaics
State-of-the-art
Nanostructured materials for TPV

Modelling and simulation toolbox
Thermal radiation
Electrical transport
Coupling

Research pathways and modelling challenges

Photovoltaics vs. thermophotovoltaics

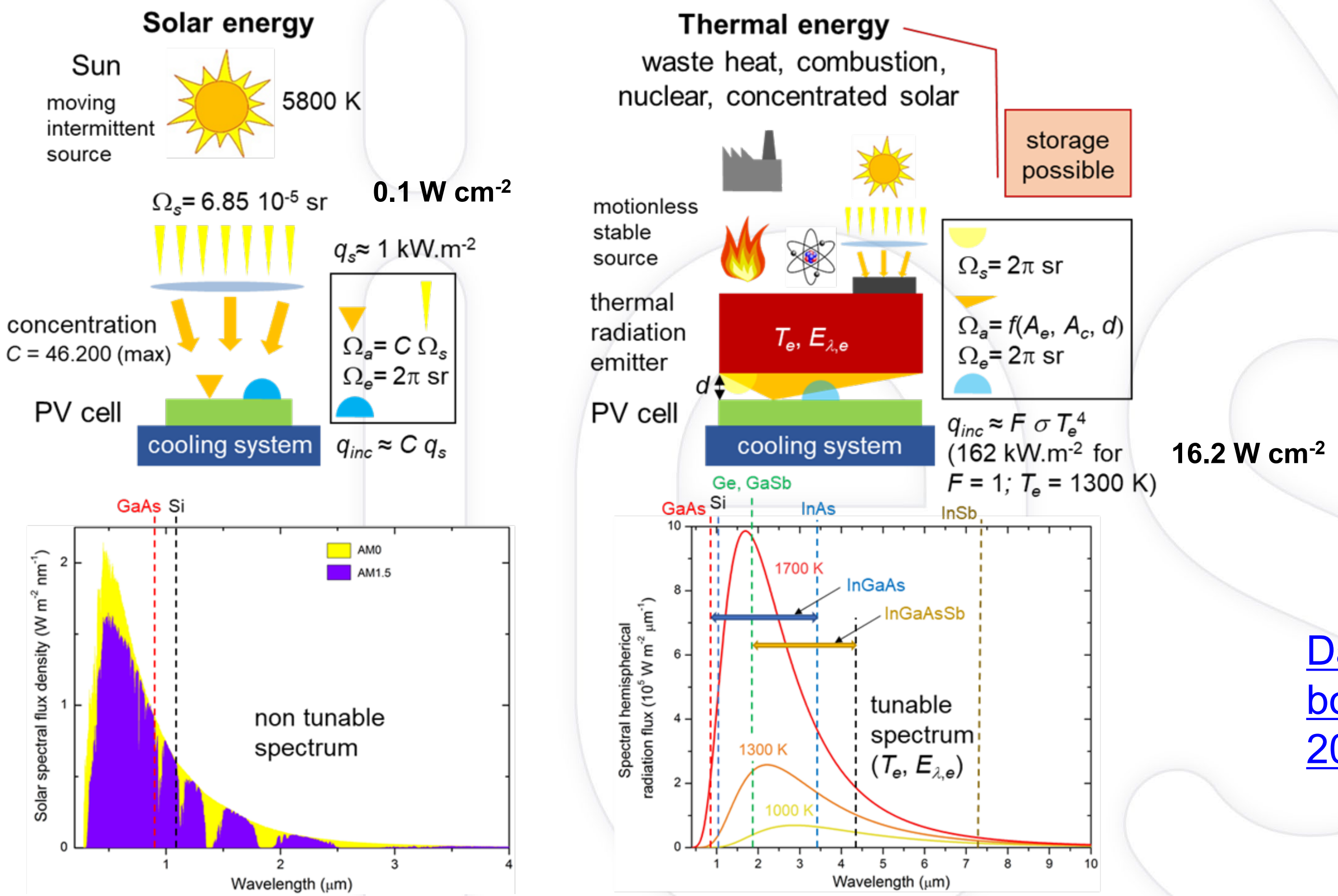

[Datas & Vaillon, book chapter, 2020]

TPV: PV conversion of (infrared) thermal radiation

Major differences between TPV and PV

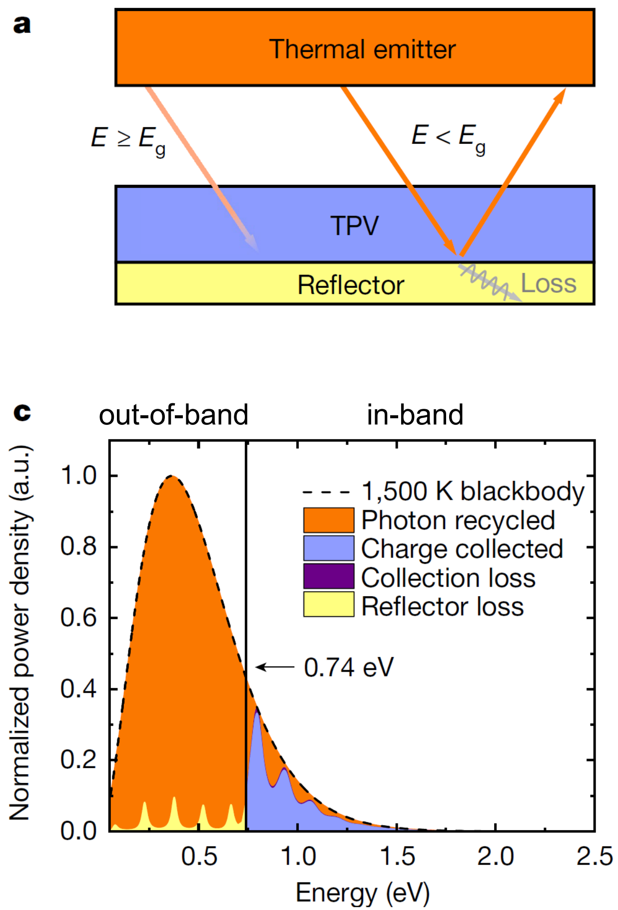

reflection
+
emission
(thermal + luminescence)

by the cell

recycled by the emitter

Fan et al., Nature, 2020

TPV: photon recycling towards the radiation source

Major differences between TPV and PV

p_{out} electrical power density

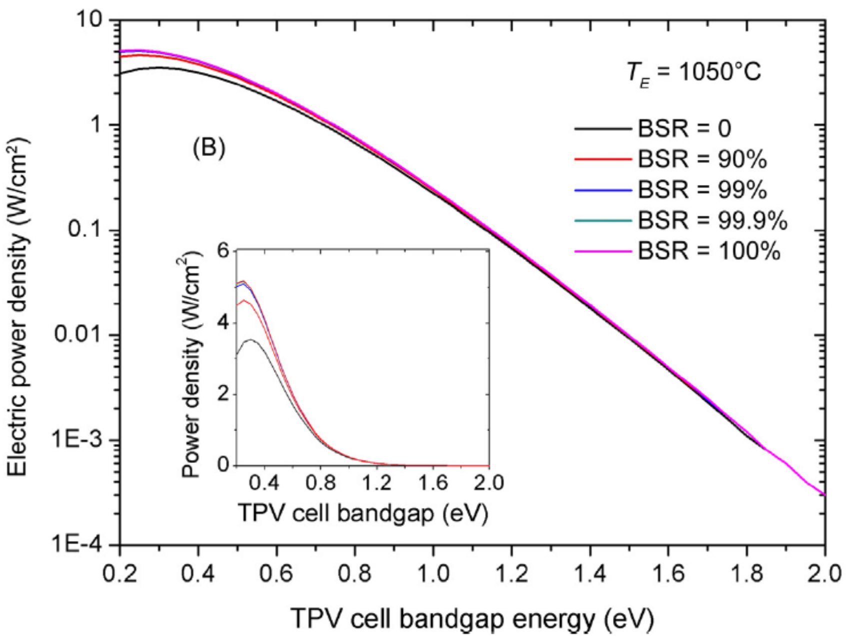

(BSR: Back Surface Reflector reflectivity of the cell; calculations, only radiative recombination)

η efficiency

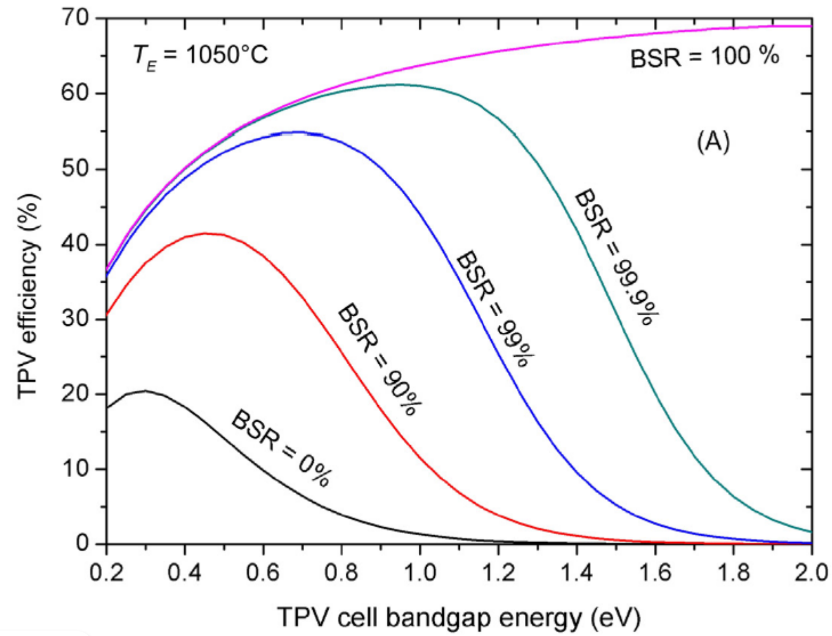

Far field

Datas & Vaillon, book chapter, 2020

Major impact of reflecting out-of-band photons

Major differences between TPV and PV

The spectrum of the radiation source can be tuned

optimum emissivity

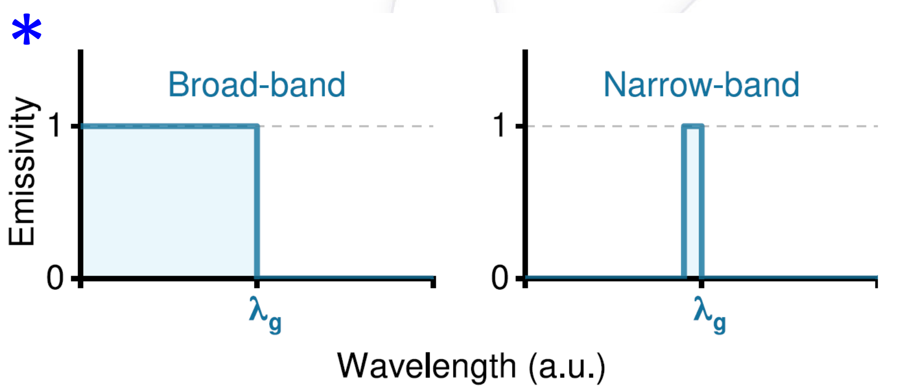

Maximizes p_{out} η

Possible additional use of a filter between the emitter and the cell

Tuning the cell reflectance and the emittance of the source

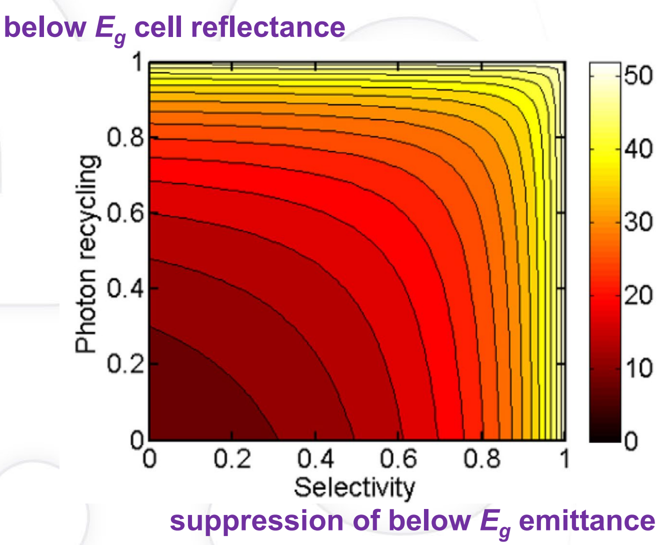

Far field

* Wang et al., SOLMAT, 2022

DeSutter et al., ECM, 2016

Major differences between TPV and PV

Examples

Selective emitter + filter

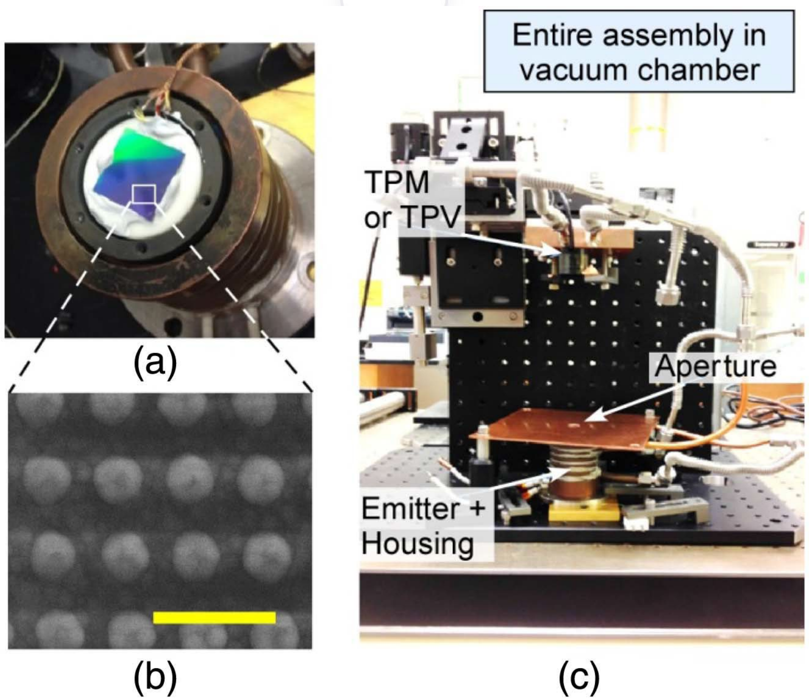

T_e = 1055 ˚C

E_g = 0.6 eV InGaAs

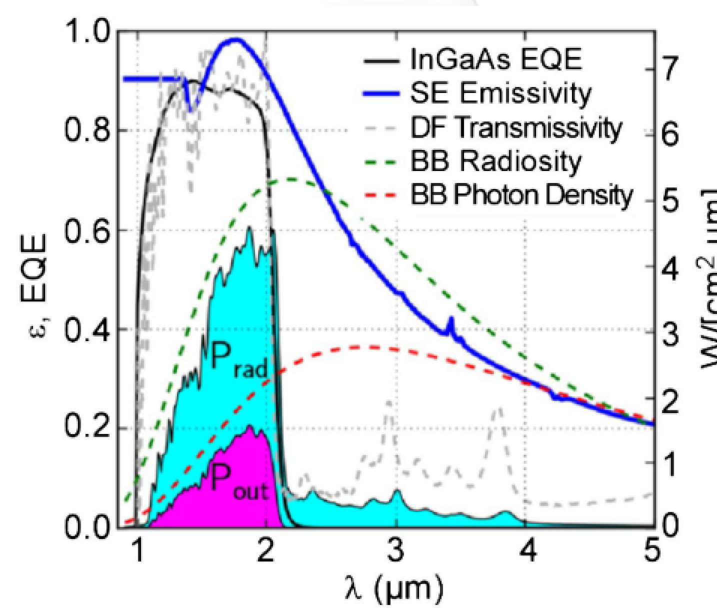

Exp.

Far field

η = 24.1%

[Woolf et al., Optica, 2018]

Major differences between TPV and PV

Examples

"Airbridge" Back Surface Reflector

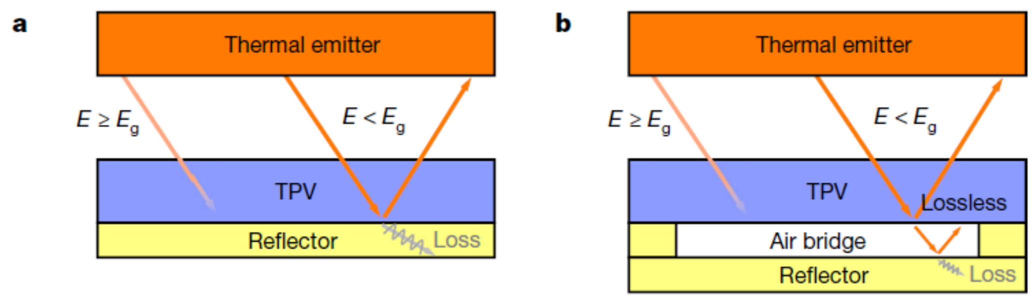

T_e ~ 1200 ˚C E_g = 0.74 eV

InGaAs

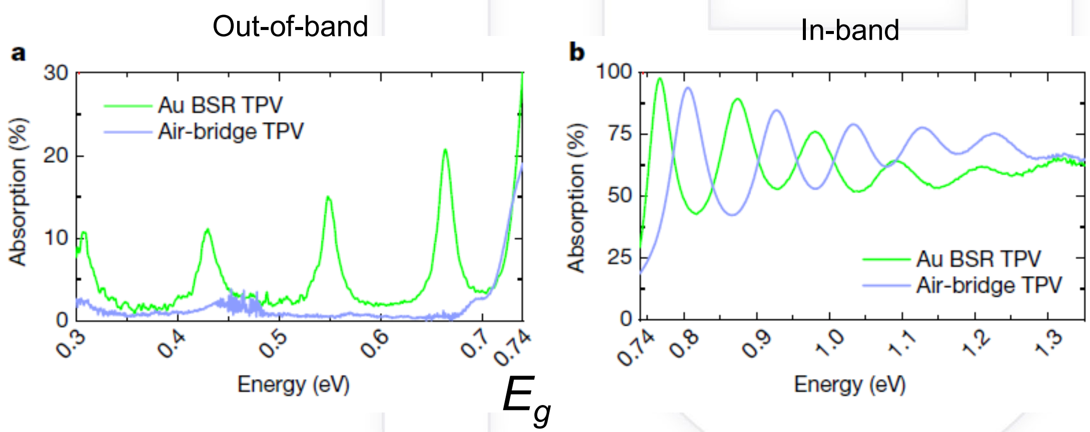

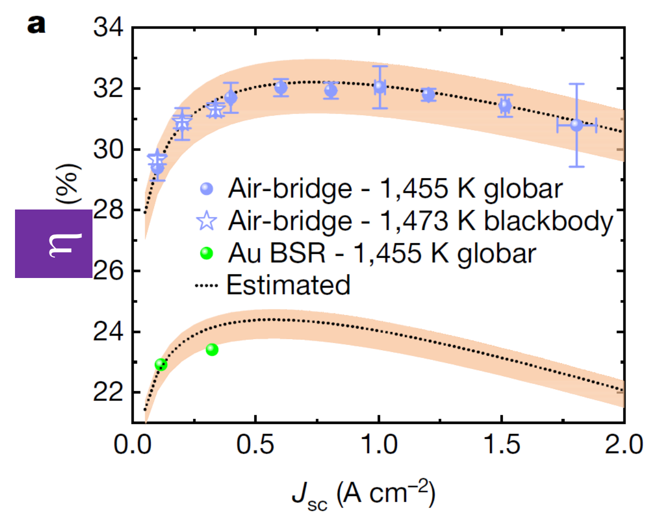

Exp. | Far field | η = 32%

Fan et al., Nature, 2020

Applications of thermophotovoltaics

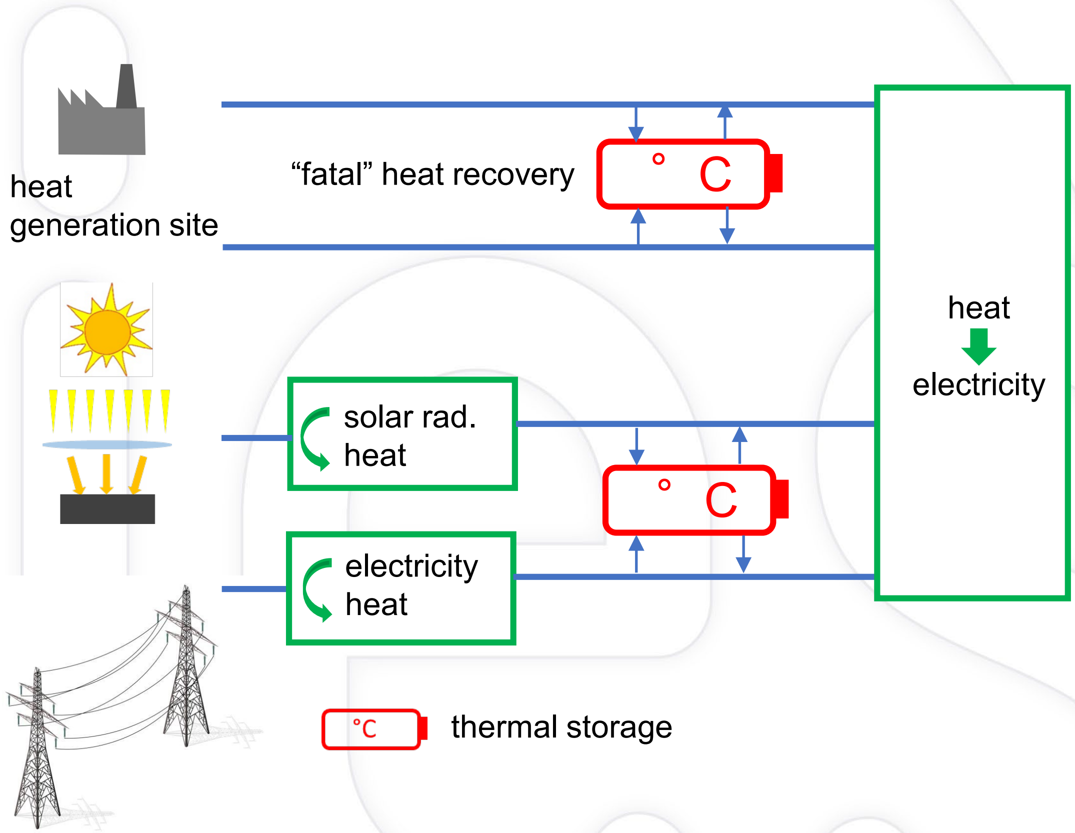

Conversion of waste or stored heat

Applications of thermophotovoltaics

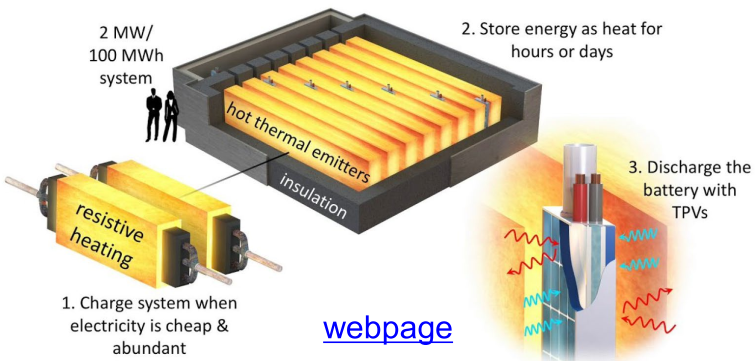

webpage

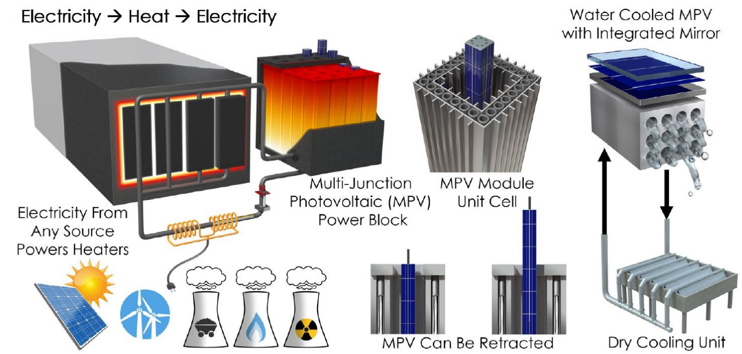

Amy et al., Appl. Energy, 2022

Thermophotovoltaic batteries

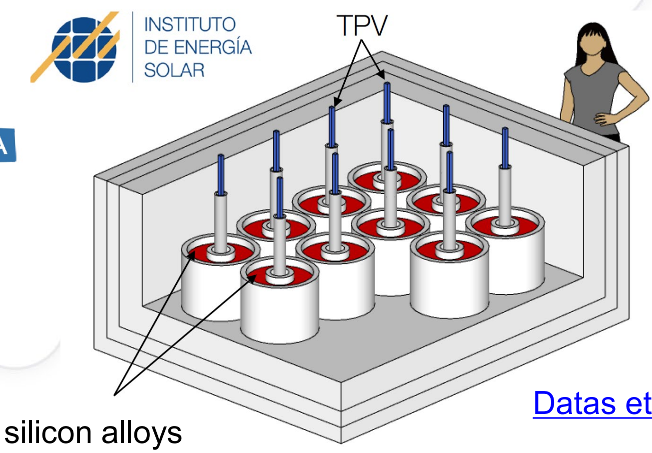

Datas et al., Joule, 2022

Losses, performance metrics

[Burger et al., Joule, 2020]

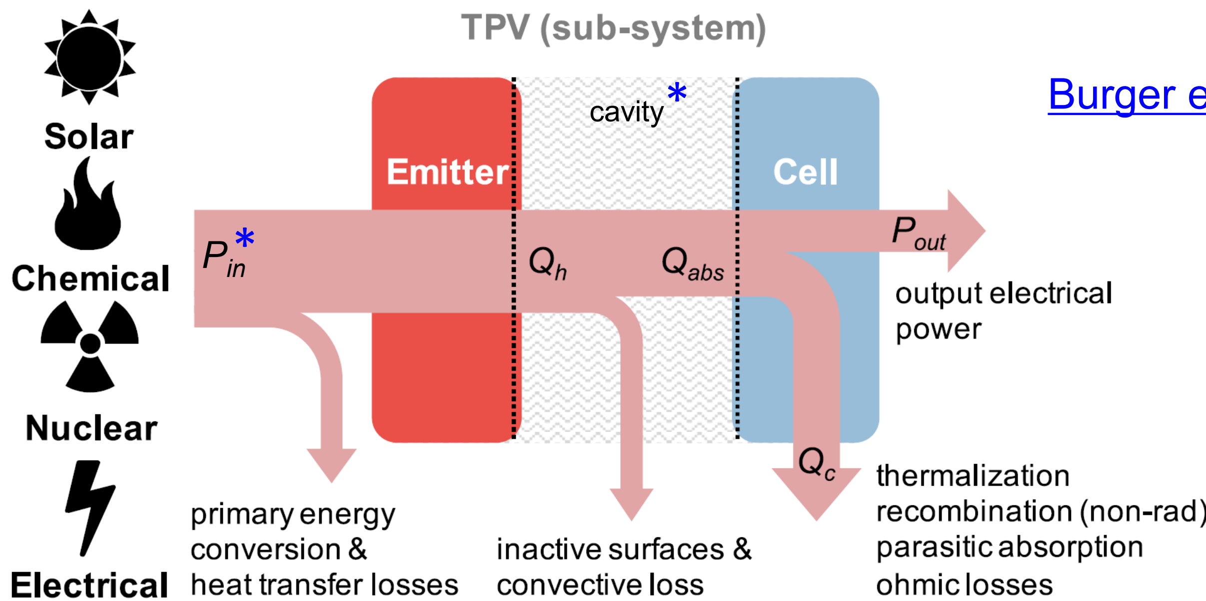

* Added to the original figure

$$p_{out} = \frac{P_{out}}{A_{cell}}$$

$$\eta_{pairwise} = \frac{P_{out}}{Q_{abs}}$$ heat absorbed by the cell

(spectral efficiency of the emitter-cell pair + conversion losses)

$$\eta_{TPV\text{-}sub} = \frac{P_{out}}{Q_h}$$ heat flow out of the emitter

(+ losses in the cavity)

$$\eta_{system} = \frac{P_{out}}{P_{in}}$$ power input to the emitter

(+ conversion and transfer losses)

"integration" losses

Various definitions of efficiency

Losses, performance metrics

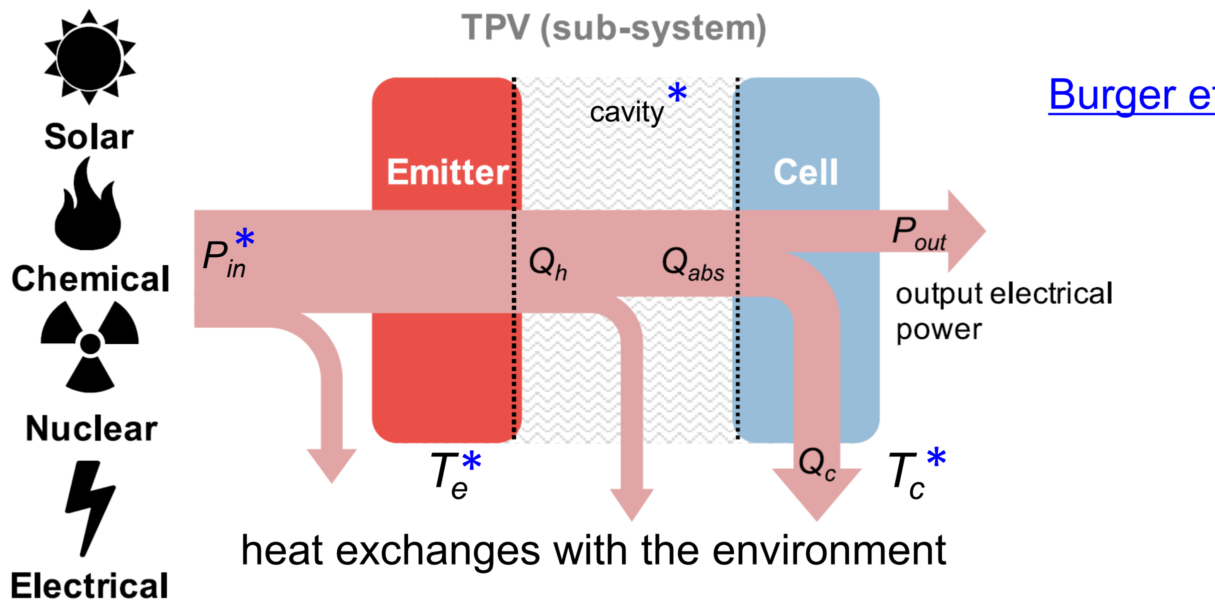

Burger et al., Joule, 2020

* Added to the original figure

$\eta_{pairwise}$ $\eta_{TPV\text{-}sub}$ η_{system} depend on T_e and T_c

Cell heating issues η_x ↓ when T_c ↑ Dupré et al., book, 2017

Thermal behavior → thermal design / management

see e.g. Blandre et al., Optics Express, 2019 Roy-Layinde et al., SOLMAT, 2022

Losses, performance metrics

$SE \cdot IQE$ [a,b] Spectral Efficiency . Internal Quantum Efficiency	$\frac{J_{sc}V_g}{Q_{abs}} = \frac{E_g \cdot \int_{E_g}^{\infty} \varepsilon_{eff}(E) \cdot IQE \cdot b(E,T_h)\, dE}{\int_0^{\infty} \varepsilon_{eff}(E) \cdot E \cdot b(E,T_h)\, dE}$
VF [c] Voltage Factor	$\frac{V_{oc}}{V_g}$
FF Fill Factor	$\frac{J_{mpp} \cdot V_{mpp}}{J_{sc} \cdot V_{oc}}$
CE Cavity Efficiency	$\frac{Q_{abs}}{Q_h}$
$\eta_{pairwise}$	$SE \cdot IQE \cdot VF \cdot FF$
$\eta_{TPV\text{-}sub}$	$SE \cdot IQE \cdot VF \cdot FF \cdot CE = \left(\frac{J_{sc}V_g}{Q_{abs}}\right)\left(\frac{V_{oc}}{V_g}\right)\left(\frac{J_{mpp}V_{mpp}}{J_{sc}V_{oc}}\right)\left(\frac{Q_{abs}}{Q_h}\right)$

Far field

$$\varepsilon_{eff} = \frac{\varepsilon_e \varepsilon_c}{\varepsilon_e + \varepsilon_c - \varepsilon_e \varepsilon_c}$$

Emittance of the cell

Emittance of the emitter

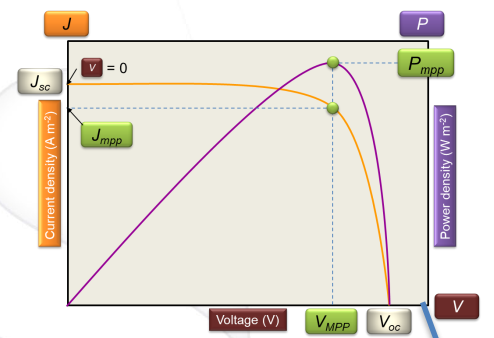

$$V_g = \frac{E_g}{q}$$

Details in Burger et al., Joule, 2020

Performance metrics = *f*(-radiation- heat transfer and electrical transport)

Record pairwise efficiencies

Single junction cells

$\eta_{pairwise}$

p_{out} < 1 W/cm^2

Wernsman et al., IEEE TED, 2004 — 23.6%
0.6 eV InGaAs TPV cell T_e = 1039 ˚C

Woolf et al., Optica, 2018 — 24.1%
0.6 eV InGaAs TPV cell T_e = 1055 ˚C

Omair et al., PNAS, 2019 — 29.1%
0.75 eV InGaAs TPV cell T_e = 1207 ˚C

Fan et al., Nature, 2020 — 32%
0.74 eV InGaAs TPV cell T_e ~ 1200 ˚C

Steiner et al., TPV-13, 2022 — 38.8%
0.74 eV InGaAs TPV cell T_e ~ 1850 ˚C

Tandem junction cells

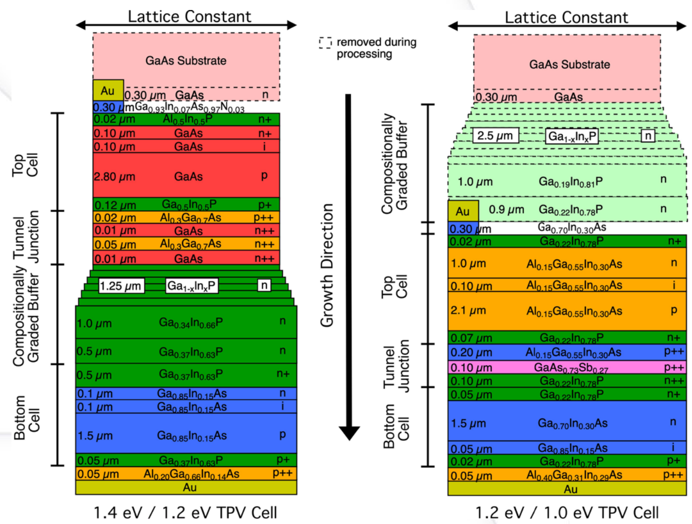

p_{out} ~ 2.39 W/cm^2 (T_e = 2400 ºC)

40% LaPotin et al., Nature, 2022

Towards 50% pairwise efficiency! But…

Record system efficiencies

Solar TPV

η_{system}

Bhatt et al., Solar Energy, 2020 — 8.4%

0.73 eV GaSb TPV cell T_e = 1403 ˚C

p_{out} ~ 1.71 W/cm^2

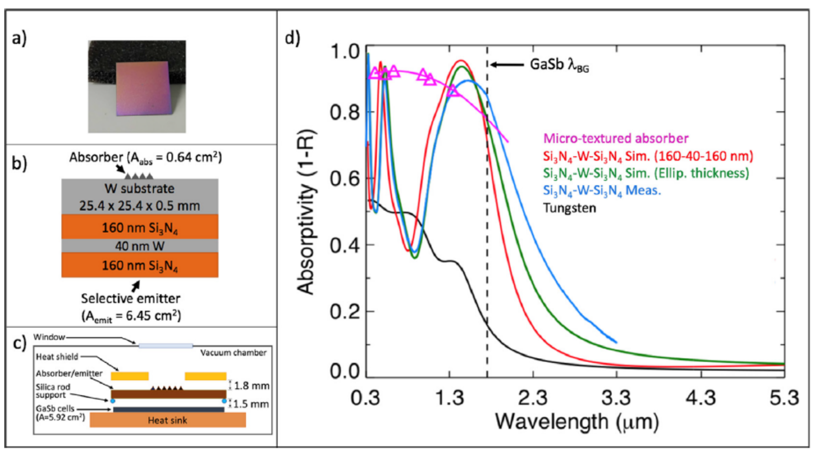

Standard TPV

11.2% — Suemitsu et al., ACS Photonics, 2020

0.7 eV InGaAs TPV cells T_e = 1065 ˚C

p_{out} ~ 0.37 W/cm^2

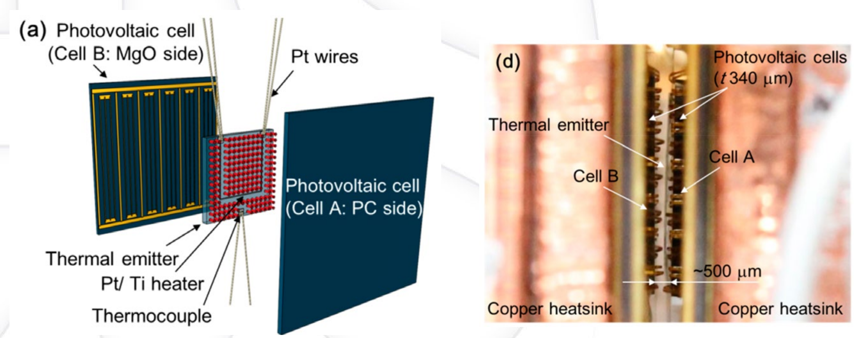

Far from the pairwise efficiency record

↑ Output power density p_{out}

Semiconductor materials for the cell

Mainstream

~0.5 - 0.8 eV: InGaAsSb, GaSb, InGaAs
with T_e ~ 1000 - 1500 °C

Woolf et al., Optica, 2018 Omair et al., PNAS, 2019

Fan et al., Nature, 2020 Steiner et al., TPV-13, 2022

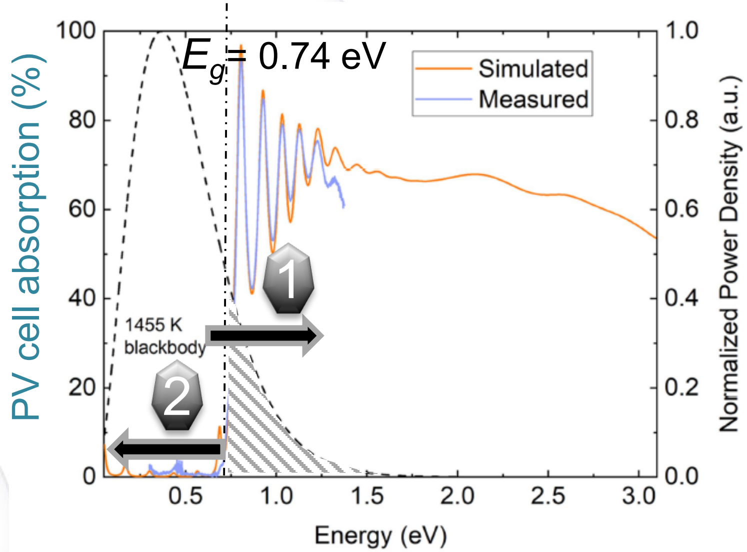

1 High bandgap (> 1 eV)
T_e > 2000 °C

GaAs (1.4 eV)
Arulanandam et al., SOLMAT, 2022

GaAs - InGaAs (1.4-1.2 eV)
AlInGaAs - InGaAs (1.2-1.0 eV)
LaPotin et al., Nature, 2022

? Si (1.1 eV) Swanson, IEEE Conf., 1980

2 Very-low bandgap (< 0.5 eV)
T_e < 1000 °C

InAs (0.36 eV)
InSb (0.17 eV)
InAs/GaSb T2SL (0.2-0.3 eV)

Yang et al., SOLMAT, 2022 Review article

↑ Output power density p_{out}

Near-field thermophotovoltaics

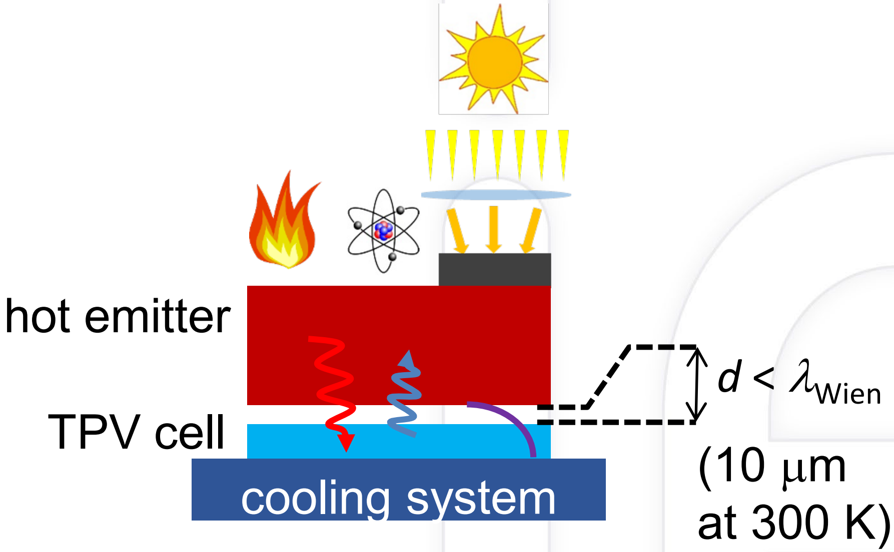

Whale & Cravalho, IEEE TEC, 2002

Tervo et al., Frontiers in Energy, 2018

Ben-Abdallah & Biehs, Z. Naturforsch., 2019

Song et al., SOLMAT, 2022

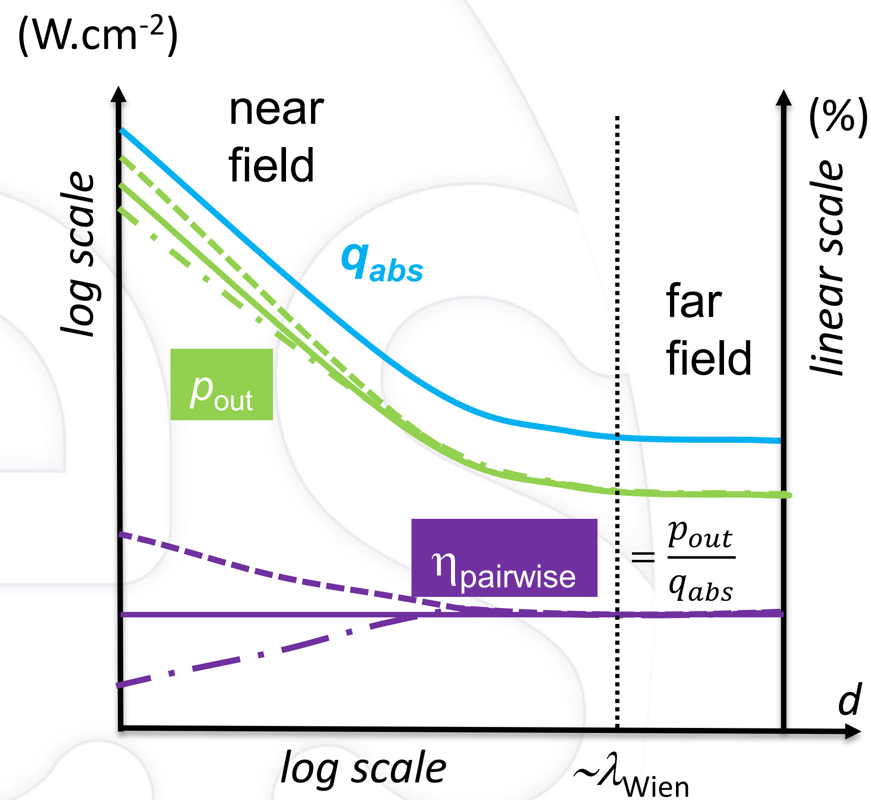

Theoretical predictions: huge near-field enhancements of the **electrical power**, the **efficiency** may go up or down

Output power density p_{out}

Dependence on T_e and E_g

Lucchesi et al., TPV-13, 2022

$$T_{Wien} \equiv \frac{E_g}{k_b}$$

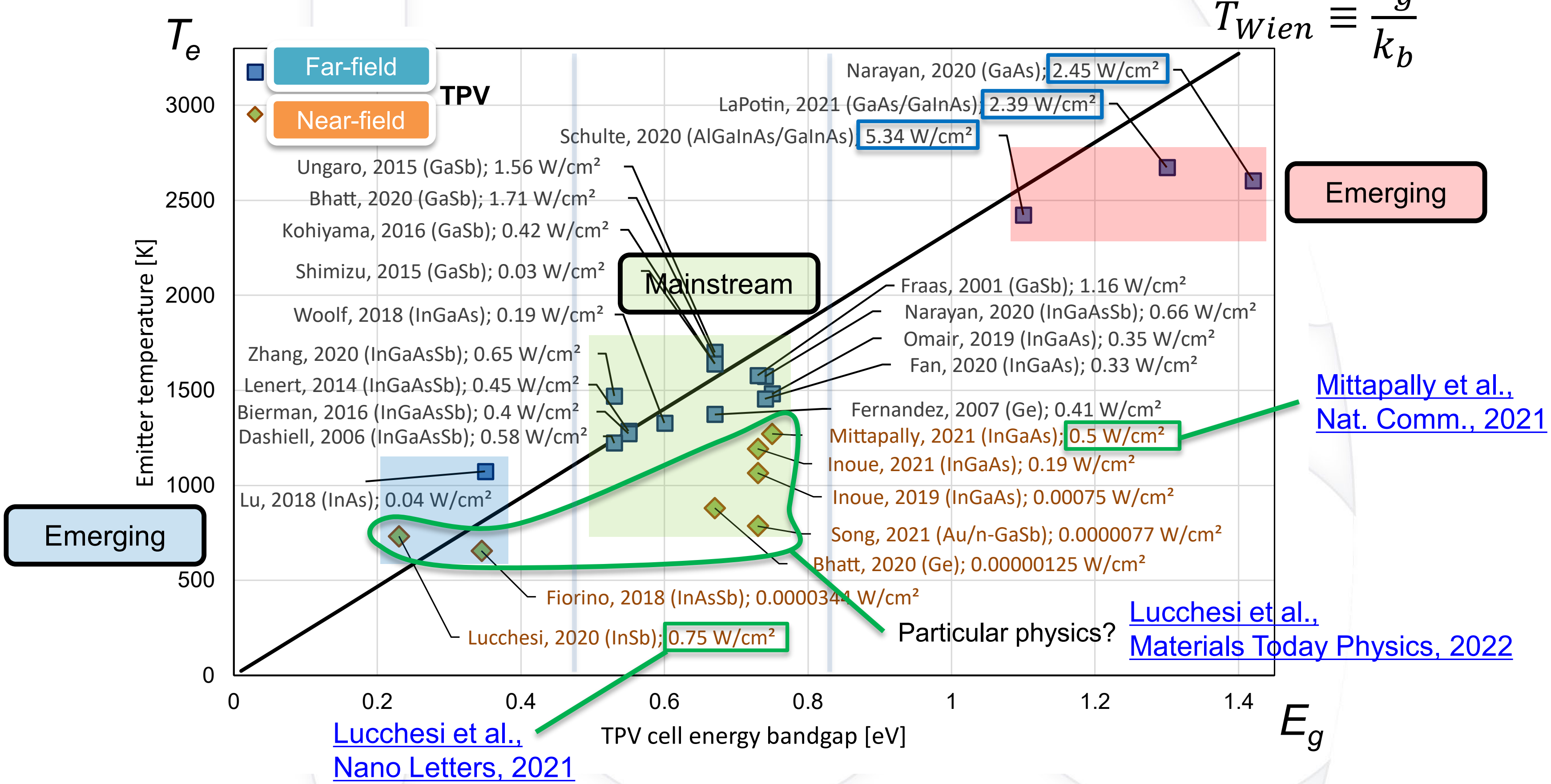

Specific limitations under high illumination?

Output power density p_{out}

Resistive losses…

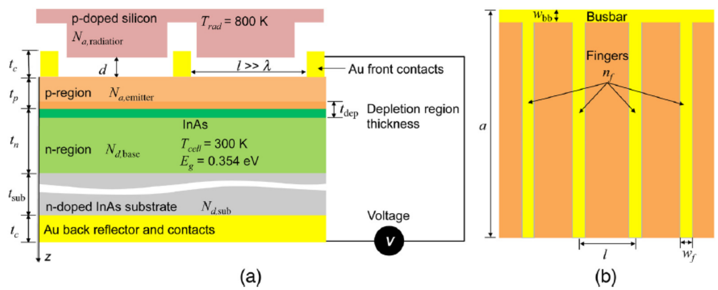

[Milovich et al., JPE, 2020]

series resistance R_s is caused by:

- lateral transport in the cell
- transport in the contact grid

front contact grid:
trade-off between shading losses and resistive losses ($R_s I^2$)

+

high illumination → high current (I)

Far field

Near field

+ high T_e

[Datas & Vaillon, Nano Energy, 2019]

T_e = 2000 K R_s = 10 mΩ A_c = 1 cm^2

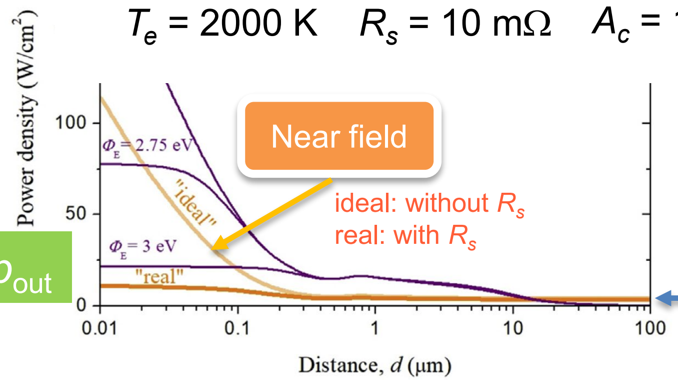

Near field

ideal: without R_s
real: with R_s

p_{out}

Far field

…"kill" the near-field radiation effects on p_{out}!

another "killer" (of η): phonon-polaritons of III-V materials
[Chen at al., APL, 2015]

Solutions to be found as in Concentrating Photovoltaics (CPV)

Nanoscales in TPV

Micro and nano-structured materials

photonic crystals | array of nanostructures metamaterials | gratings | …

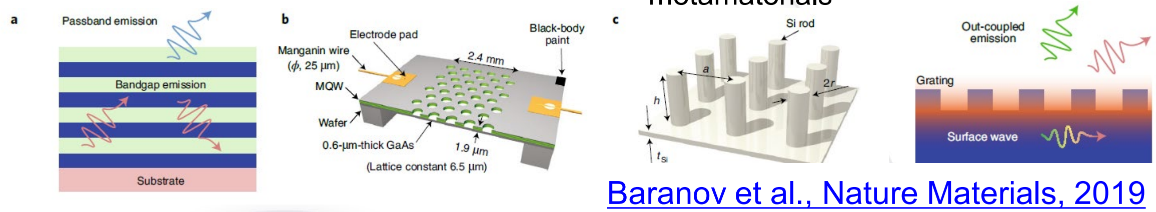

…

Baranov et al., Nature Materials, 2019

emitter

TPV cell

Near field

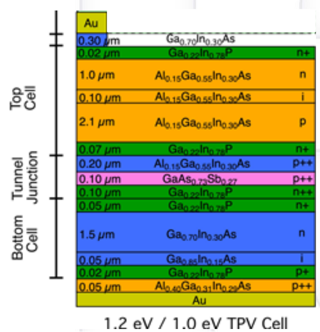

LaPotin et al., Nature, 2022

Nanophotonics

(Wednesday's lecture)

Nanoscale thermal radiation

Electrical transport in a multilayered medium

Modelling approaches and simulation tools?

Material properties & fabrication capabilities

Electrical transport properties

- bandgap (E_g)
- effective masses
- mobilities (μ)
- lifetimes (radiative, Auger, SRH)
- surface recombination velocities

literature, databases, models

see e.g. Vurgaftman et al. JAP, 2011   IOFFE website

+ majority carrier (doping) concentrations

Electromagnetic (ε) / optical (m) / radiative (κ) properties

complex permittivity $\varepsilon = \varepsilon' + \mathrm{i}\ \varepsilon''$

complex refractive index $m = n + \mathrm{i}\ k$

+ Kramers-Kronig relation $\kappa = \dfrac{4\pi\ k}{\lambda}$

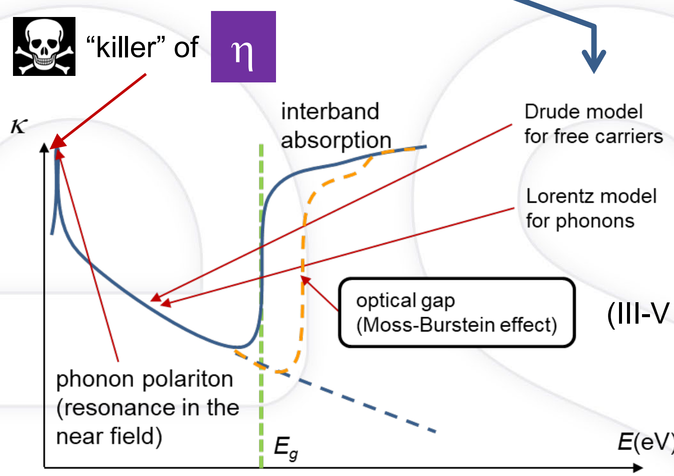

(III-V semiconductors)

see e.g. Vaillon et al., Optics Express, 2019   Milovich et al., JPE, 2020

Questions to ask yourself

- Can the structure be functional at the selected temperature?
- Aren't the contacts on the cell missing?
- Can the structure be fabricated?

ATTENTION

Strong bases required for meaningful simulations

Far field

Selective emitters for TPV

Selectivity

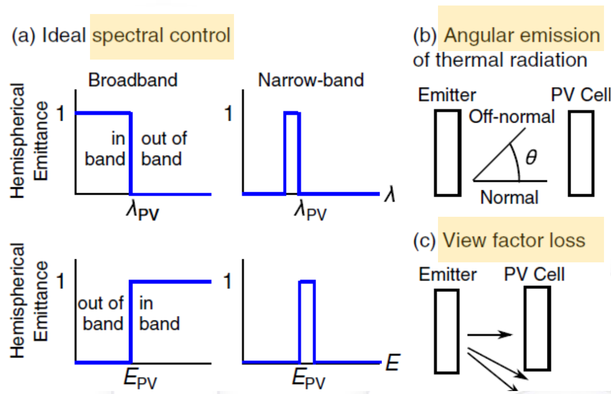

Sakakibara et al., JPE, 2019

+ Pfiester & Vandervelde, PSSa, 2016

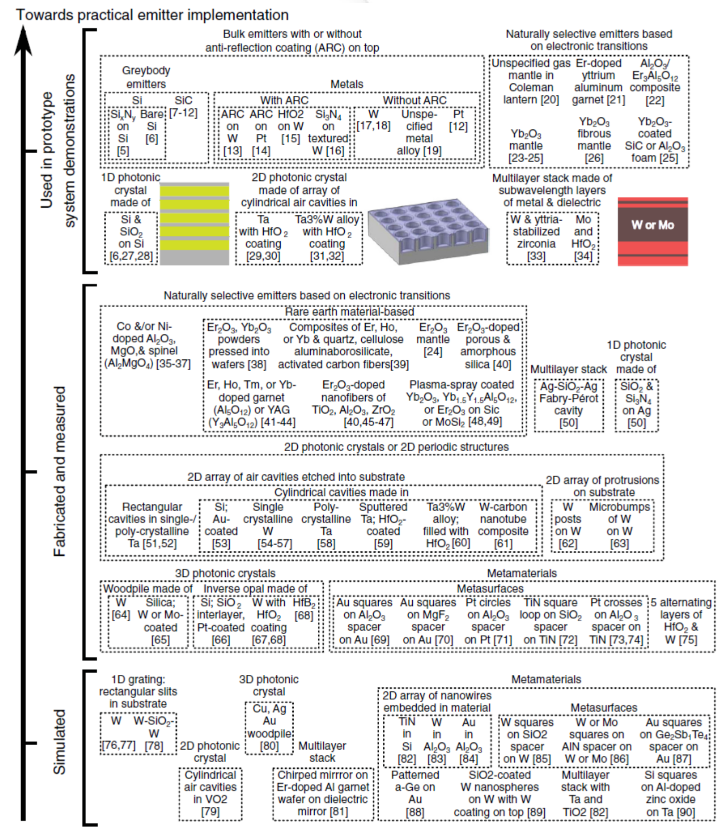

Materials and structures

Wang et al., SOLMAT, 2022

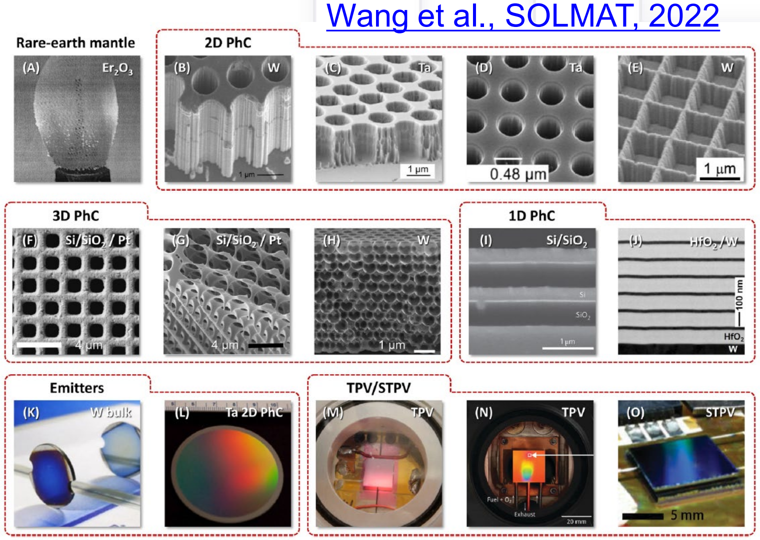

(spectral; directional / hemispherical) emittance?

Selective emitters and cells for TPV

Far field

calculation of emittance

ε_e

ε_c

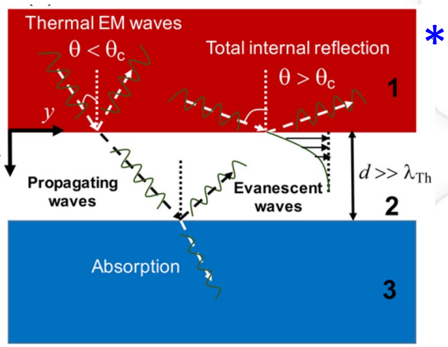

*

reflections in the cavity

$$\varepsilon_{eff} = \frac{\varepsilon_e \varepsilon_c}{\varepsilon_e + \varepsilon_c - \varepsilon_e \varepsilon_c}$$

effective emittance of the emitter-cell pair

Kirchhoff
emittance = absorptance

⬇

Rigorous Coupled Wave Approximation (RCWA)

+…

Near field

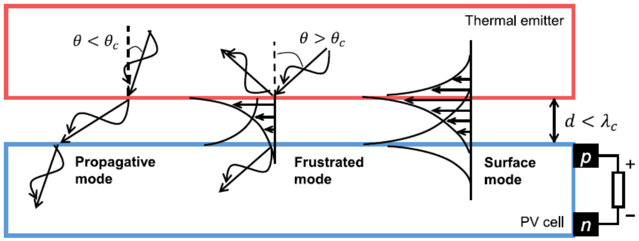

[Song et al., SOLMAT, 2022]

full calculation of radiation exchange in the emitter-cell system

(Wednesday's lecture) ⬇

Fluctuational Electrodynamics (FE)

Methods

Transfer/Scattering-matrix

Finite Difference Time Domain (FDTD)

Based on discrete dipoles

Boundary Element Method (BEM)

+…

see e.g. [Francoeur, book chapter, 2017] * [Cuevas & Garcia-Vidal, ACS Photonics, 2018]

Three usual models (1)

Detailed Balance (DB) model

[Shockley & Queisser, JAP, 1961](#)

Generation
Recombination

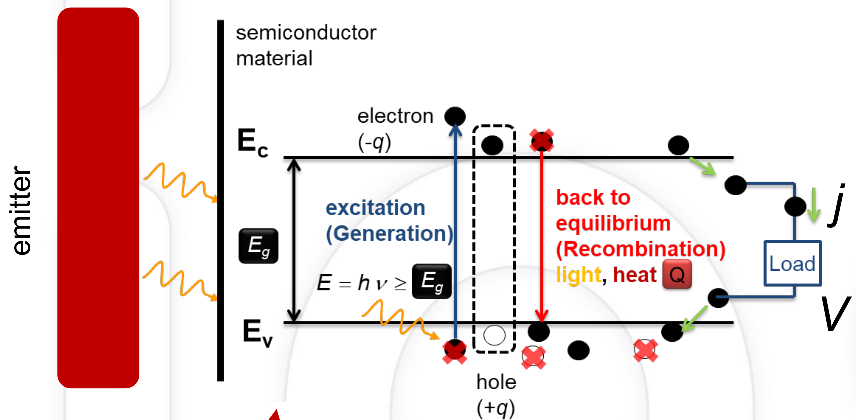

$p_{out} = j(V)\, V$

see details in e.g.

[Datas & Algora, SOMAT, 2010](#)

[DeSutter et al., PR Applied, 2017](#)

[Song et al., SOLMAT, 2022](#)

rate of photons **absorbed** generating e-h pairs

current density

rate of e-h pair **Recombination**

$$j(V) = q\{G_a - [R_e(V) + R_{nrr}(V)]\}$$

voltage

rate of **nonradiative** recombination (Auger, Shockley-Read-Hall, surface)

rate of e-h pair **Generation**

rate of photons **emitted** by **radiative Recombination** leaving the cell (external luminescence)

radiation model

electrical model

No information about local quantities in the cell

Three usual models (2)

Governing equations with local quantities

Sze et al., book, 1985 (1st ed.)-2021 (4th ed.)

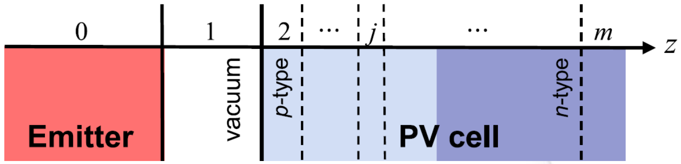

Song et al., SOLMAT, 2022

1D Blandre et al., Scientific Reports, 2017

		drift / diffusion
n current	(electrons)	$J_n(z) = e\, n(z)\mu_n E(z) + e\, D_n \frac{dn}{dz}$
p current	(holes)	$J_p(z) = e\, p(z)\, \mu_p\, E(z) - e\, D_p \frac{dp}{dz}$
Poisson's equation		$\frac{dE}{dz} = -\frac{d^2V}{dz^2} = -\frac{e}{\varepsilon}[n(z) - p(z) + N_a(z) - N_d(z)]$
continuity eq. for n		$-\frac{1}{e}\frac{dJ_n(z)}{dz} = G(z) - R(z)$
continuity eq. for p		$\frac{1}{e}\frac{dJ_p(z)}{dz} = G(z) - R(z)$
photo-generation rate		$G(z) = \int_0^\infty \kappa_\omega^{IB} \frac{q_\omega^{inc}(z)}{\hbar\omega} d\omega$
recombination rate		$R(z) = R_{rad}(z) + R_{Auger}(z) + R_{SRH}(z)$
radiative recombination rate		$R_{\mathrm{rad}}(z) = B(n(z)p(z) - n_i^2)$
Auger recombination rate		$R_{\mathrm{Auger}}(z) = C_n n(z)(n(z)p(z) - n_i^2) + C_p p(z)(n(z)p(z) - n_i^2)$
SRH recombination rate		$R_{\mathrm{SRH}}(z) = \frac{n(z)p(z) - n_i^2}{\tau_p^{\mathrm{SRH}}(n(z) + n_i \exp[(E_t - E_i)/k_bT]) + \tau_n^{\mathrm{SRH}}(p(z) + n_i \exp[(E_t - E_i)/k_bT])}$
surface recombination		$R_{\mathrm{surf}}(z_s) = \frac{S_n S_p (n(z_s)p(z_s) - n_i^2)}{S_n(n(z_s) + n_i) + S_p(p(z_s) + n_i)}$

(rem: notation e for q the elementary charge)

Simulation codes

Sentaurus	2D, 3D
Atlas	2D, 3D
CoBoGui	2D, 3D
Quokka2	1D, 2D, 3D
Quokka3	1D, 2D, 3D
PC3D	3D
PC1D	1D
I2E (+PC1D)	1D
SCAPS	1D
ADEPT	1D
OPV Lab	1D
Setfos	1D
QS Cell	1D
SARAH (IBC)	1D, 2D
wxAMPS	1D
gpvdm	1D
Mxcad (ies l'institut d'électronique)	1D

Parola et al., SOLMAT, 2019

https://www.pvlighthouse.com.au/simulation-programs

Poisson-Drift-Diffusion (PDD) model

Three usual models (3)

The low-injection approximation

Green, book, 1982

Song et al., SOLMAT, 2022

- **concentration of photogenerated carriers is much lower than the doping**
- electric field and recombination independent of the e-h pair generation rate
- local recombination rate $R(n) = \frac{\Delta n(z)}{\tau_n}$ ← local excess of minority carriers; ← uniform carrier lifetime $\qquad R(p) = \frac{\Delta p(z)}{\tau_p}$

2 linear (diffusion of e in the p-region, of h in the n-region) **non-coupled** differential equations

$$D_n \frac{d^2 \Delta n(z)}{dz^2} + G(z) - \frac{\Delta n(z)}{\tau_n} = 0$$

$$D_p \frac{d^2 \Delta p(z)}{dz^2} + G(z) - \frac{\Delta p(z)}{\tau_p} = 0$$

Diffusion Generation Recombination

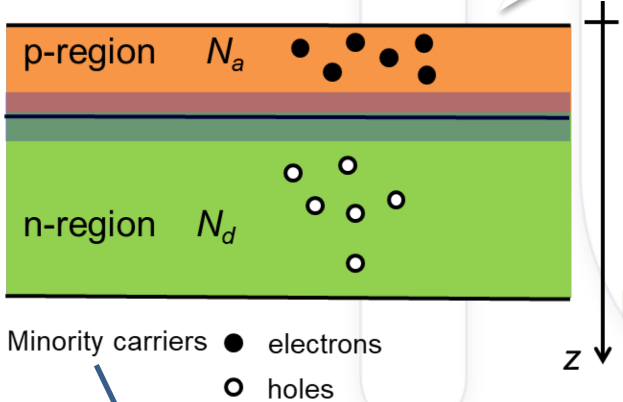

Minority Carrier Separation (MCS) model

Luminescence and photon recycling

In-band photon recycling

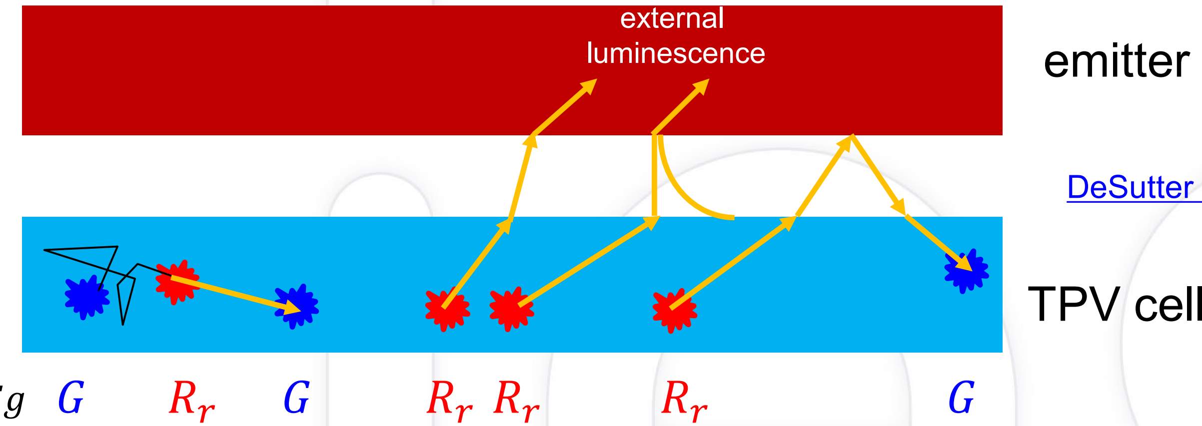

[DeSutter et al., PR Applied, 2017]

Generation **Recycling** **Recycling**

Radiative Recombination = internal luminescence

internal luminescence
generalized Planck radiation law
[Würfel, JPCSSP, 1982]

Radiation transfer – electrical transport coupling

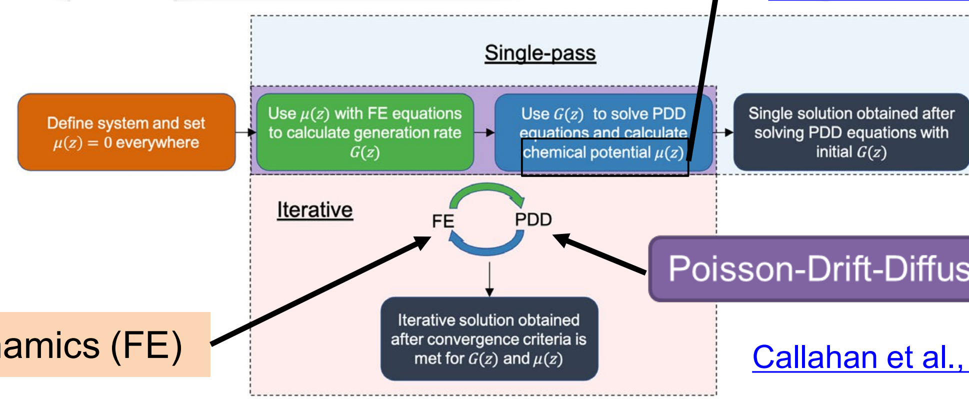

Poisson-Drift-Diffusion (PDD) model

Fluctuational Electrodynamics (FE)

[Callahan et al., PR Applied, 2021]

Luminescence and photon recycling

Impact of evanescent modes on external luminescence

"radiative limit"

external luminescence / total recombination

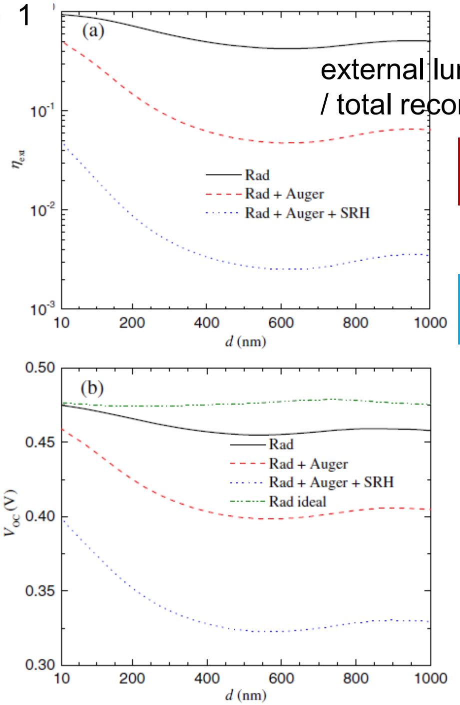

FE + DB models

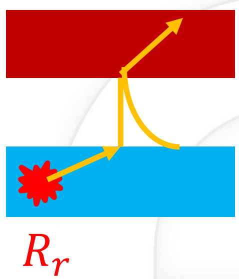

Near field effects

FIG. 6. (a) Cell external luminescence efficiency (η_{ext}) and (b) open-circuit voltage (V_{OC}), as a function of the gap thickness (d) for the case of the Si emitter, when only radiative (Rad), intrinsic (Rad + Auger), and all (Rad + Auger + SRH) recombination processes are considered. The open-circuit voltage in the ideal case of the radiative limit with no luminescence towards the substrate (Rad ideal) is plotted in panel (b).

DeSutter et al., PR Applied, 2017

Impact of the coupling

iterative (FE + PDD) models   Callahan et al., PR Applied, 2021

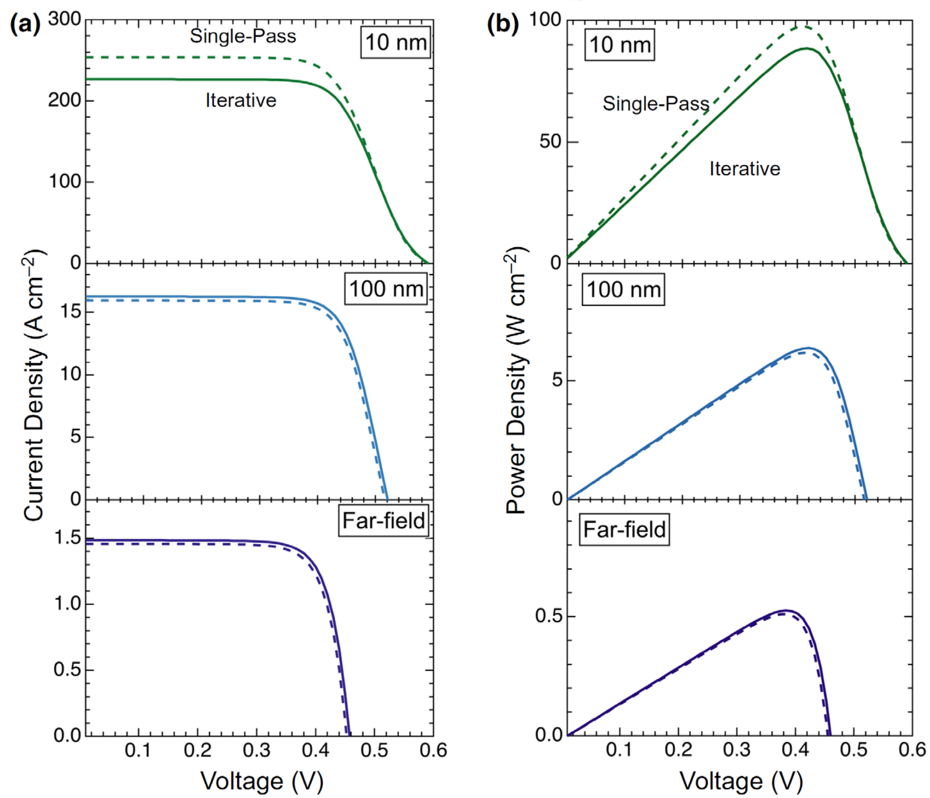

In the (very) near field!

Contacts and quasi-perfect reflection

Back Contacts

Airbridge

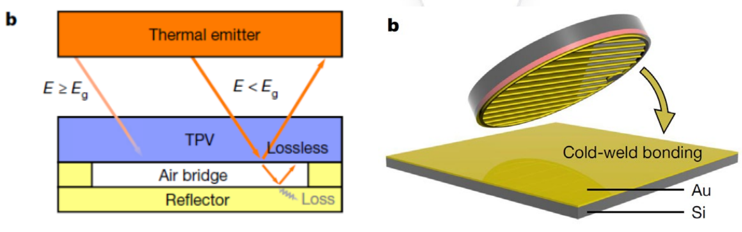

[Fan et al., Nature, 2020]

Patterned Dielectric

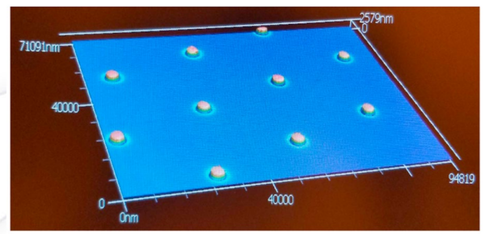

[Arulanandam et al., SOLMAT, 2022]

Interdigitated

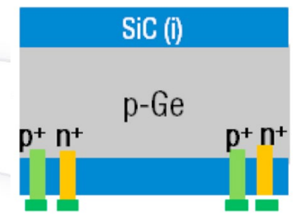

“IBC” TPV cell

[Jimenéz et al., SOLMAT, 2022]

?

New structures to achieve quasi-perfect reflection

⬇

2D – 3D radiation modeling

e.g. RCWA calculations in [Arulanandam et al., IEEE PVSC, 2021]

+ front contact grid

Far field

Near field

Resistive losses

Resistive and shading losses

?

New structures to ↓ the resistive losses and the shading losses

↓ I (current)

Multi-junction cells

Rey-Stolle et al., book chapter, 2016

Monolithic Interconnected Modules (MIM)

Datas & Linares, RSER, 2017

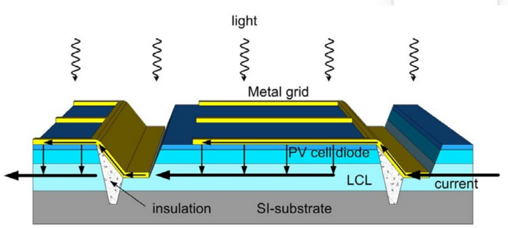

↓ R_s (series resistance)

Micro cells

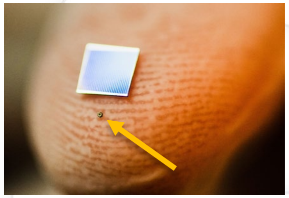

PV magazine, 2021

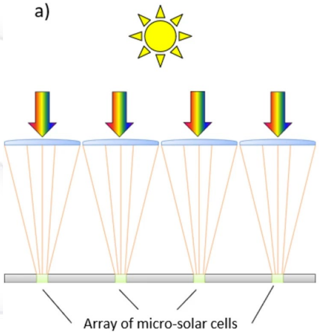

Siopa et al. Sci. Reports, 2020

Near-field TPV

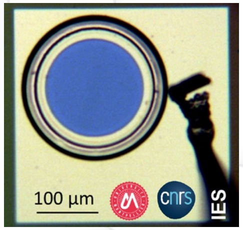

Vaillon et al., Optics Express, 2019

Cakiroglu et al., SOLMAT, 2019

Interdigitated Back Contact (IBC) cells

Verlinden, book chapter, 2016

TPV Jimenéz et al., SOLMAT, 2022

Transparent Conducting Electrode (TCE)

Near-field TPV Theo.

Karalis & Joannopoulos, Sci. Reports, 2017

Karalis & Joannopoulos, Proc. of SPIE, 2019

Adapted modelling of radiation transfer and electrical transport

Hybrid thermionic-thermophotovoltaic (TiPV) device

? ↓ resistive and shading losses and ↑ thermal energy conversion

*

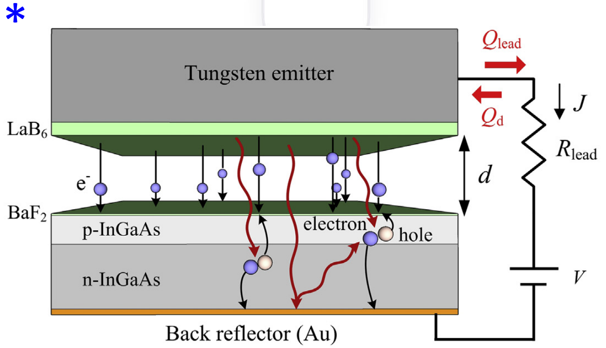

*

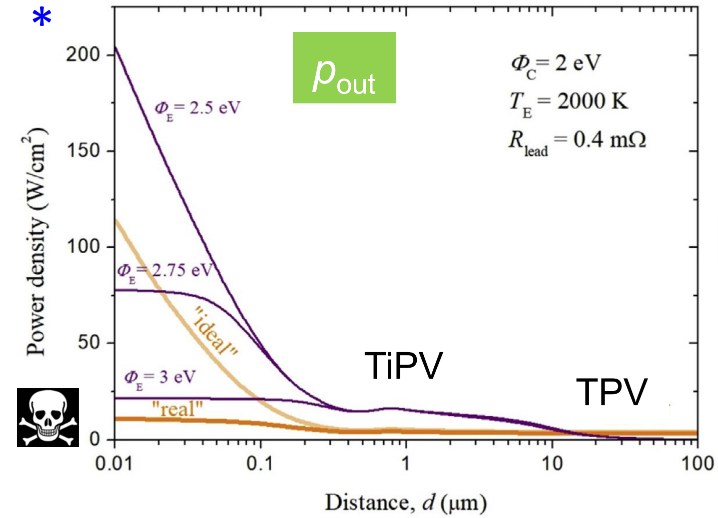

Theo.

Far field | Theo. | Datas, APL, 2016

Near field | Theo. | * Datas & Vaillon, Nano Energy, 2019 | Liao et al., APL, 2019

~~Exp.~~

Far field | Exp. | Bellucci et al., Adv. Energy Mater., 2022 | Bellucci et al., SOLMAT, 2022

⬇

Finding materials and structures that allow both conversions in an optimal way

Very-low bandgap TPV cells

?

TPV at low emitter temperatures?

IR photodetectors and lasers ➡ TPV cells

Rationale

E_g (eV) @ 300 K | ~0.75 | 0.36 | 0.17

InGaAs InAs InSb

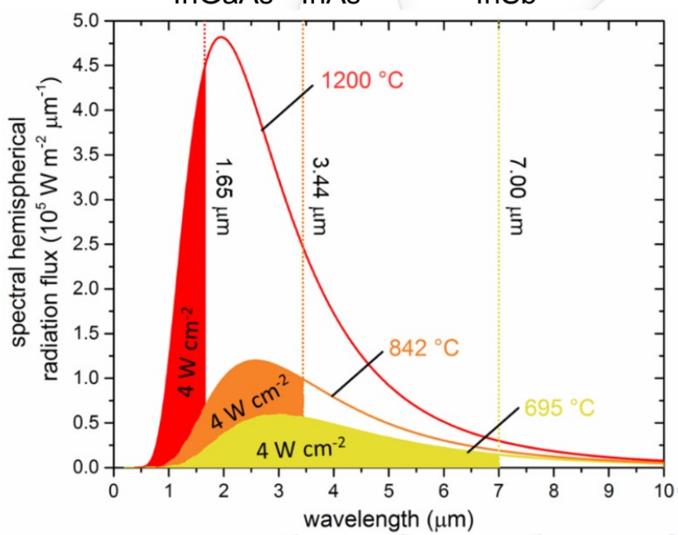

Example of InAs/GaSb T2SL (E_g = 0.2-0.3 eV)

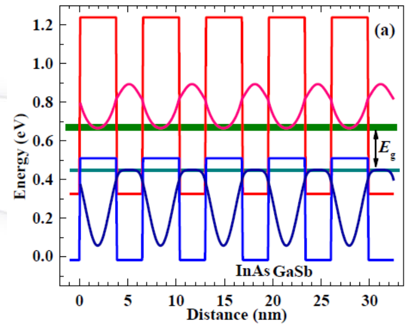

Band structure: minibands

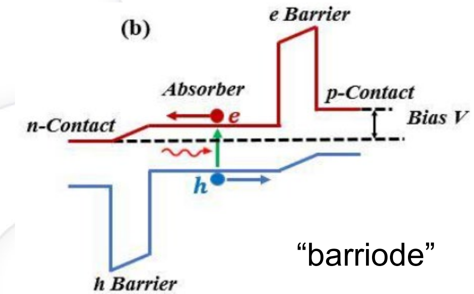

"barriode"

[Huang, Ph.D. dissertation, 2020]

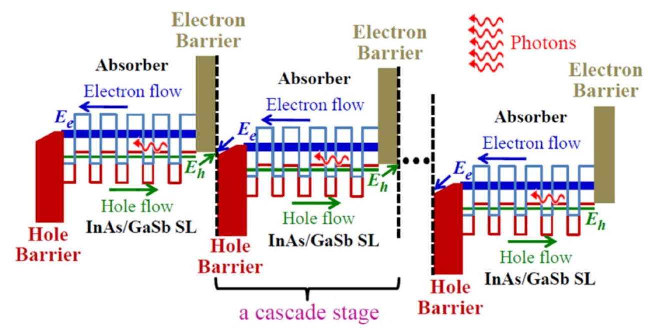

Interband Cascade PV structure

[Yang et al., SOLMAT, 2022]

Review article

⬇ ⬇

Simulations to optimize materials and structures

➡ InAs/InAsSb T2SL

anr® [LOW-GAP-TPV] (2021-2025)

Thermophotonics (TPX)

? **TPV at very low emitter temperatures?**

Concept proposed by
Harder & Green, IOP SST, 2003

*

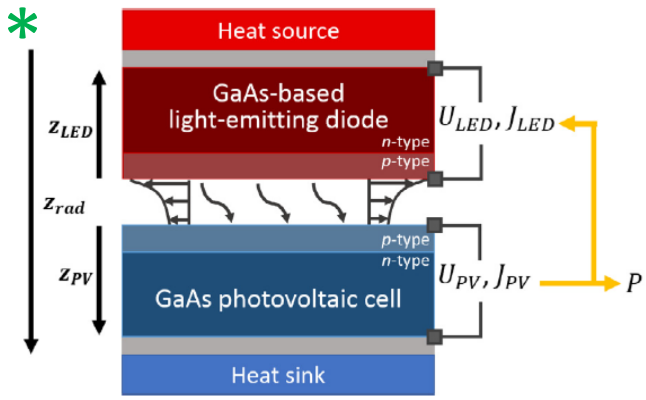

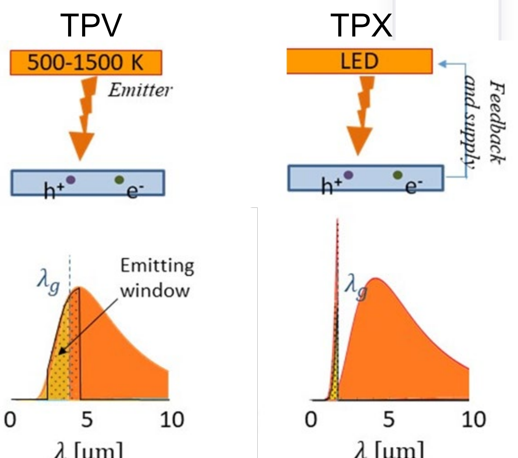

Chapuis et al., Photoniques, 2020

*

p_{out}

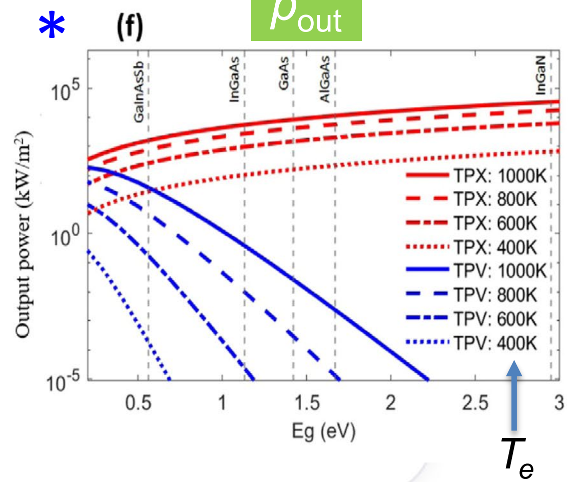

$\eta_{pairwise}$ T_e = 600 K

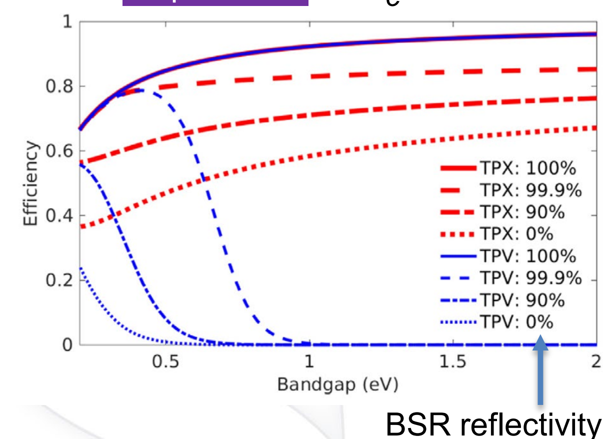

Theo. | Far field | * Sadi et al., SOLMAT, 2022

Theo. | Near field | * Legendre & Chapuis, SOLMAT, 2022

~~Exp.~~

⬇

Modelling to find the optimum materials and structures

Thermal management and optical cavities

$\eta_{pairwise}$ = 40% η_{system} = 11.2% ? ↑ system efficiency?

Thermal losses

Example of a solar TPV system

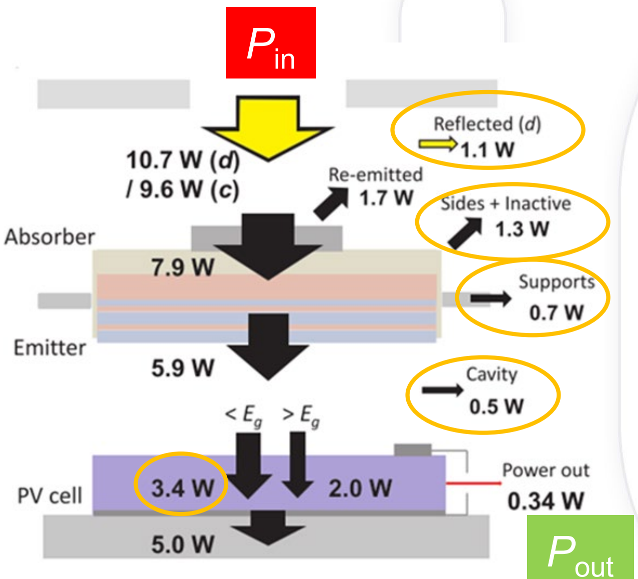

Lenert et al., Nature Energy, 2014

Ideal regenerative

Omair et al., PNAS, 2019

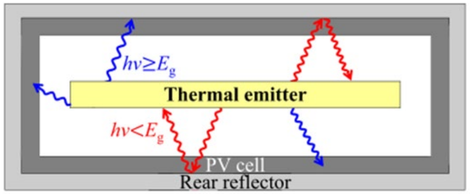

Optical cavities

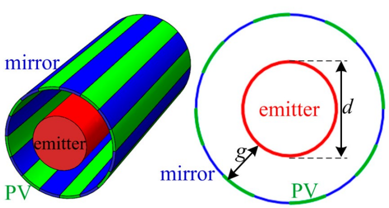

Zhou et al., Energies, 2016

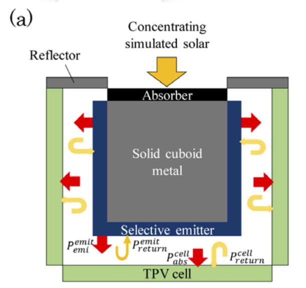

Kohiyama et al., Optics Express, 2020

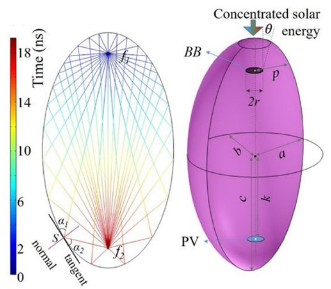

Talebzadeh et al., IEEE JPV, 2022

Modelling of the full system from P_{in} to P_{out}

Acknowledgments

Collaborators over the years

Dilek Cakiroglu, Philippe Christol, Frédéric Martinez, Stéphanie Parola, Jean-Philippe Perez, Basile Roux, Thierry Taliercio, Eric Tournié

Etienne Blandre, Olivier Chapuis, Olivier Dupré, Julien Legendre, Christophe Lucchesi, Olivier Merchiers

Etienne Blandre (again), Jérémie Drevillon

Elisa Antolin, Alejandro Datas, Antonio Marti, Juan Villa

Martin Green

Michael Bernardi, John DeSutter, Mathieu Francoeur, Daniel Milovich

INSIS – Project team « TREE »

Funding

ANR-11-EQPX-0016, ANR-16-IDEX-0005, ANR-16-CE05-0013, ANR-18-CE24-0019, ANR-21-CE50-0018

Networking

INSIS – Project team « TREE »

GDR NAME & TAMARYS

iTPV

international R&D network on ThermoPhotoVoltaics
website

Additional slides

Thermal-to-electrical energy converters

In space applications

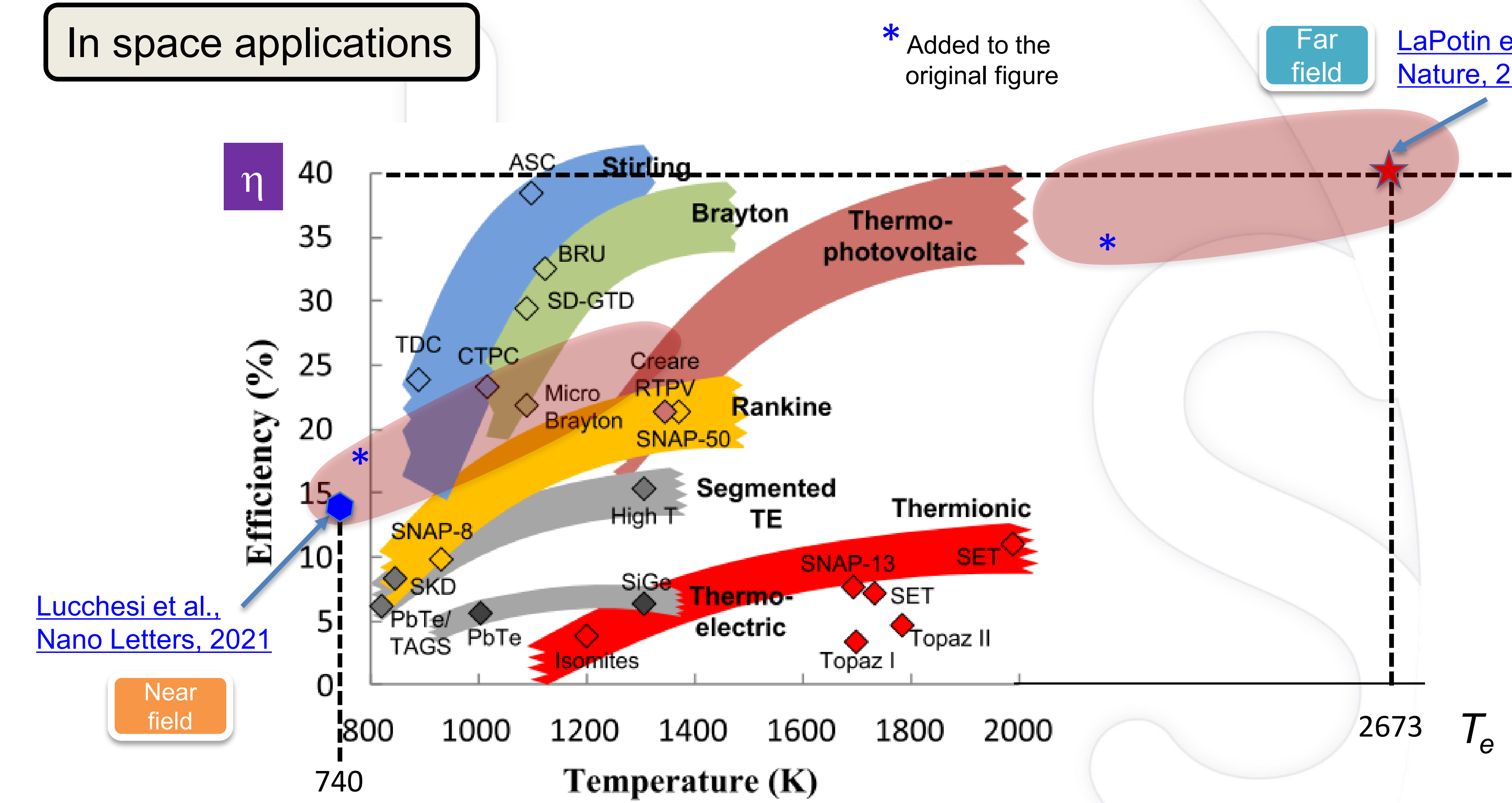

Datas & Marti, SOLMAT, 2017

Major differences between TPV and PV

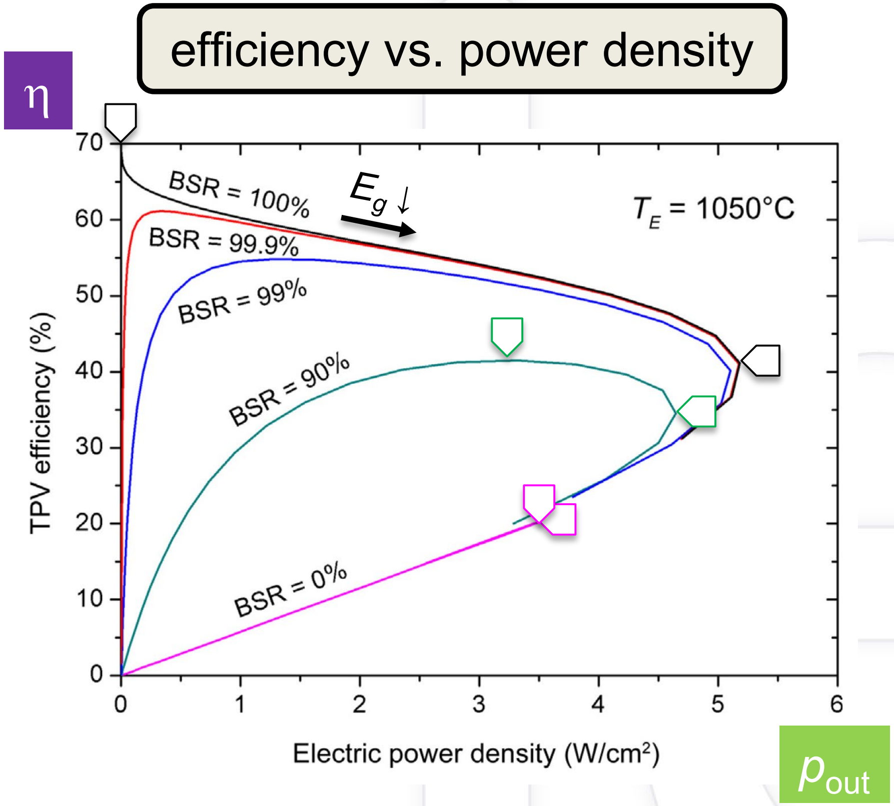

(BSR: Back Surface Reflector reflectivity of the cell; calculations, only radiative recombination)

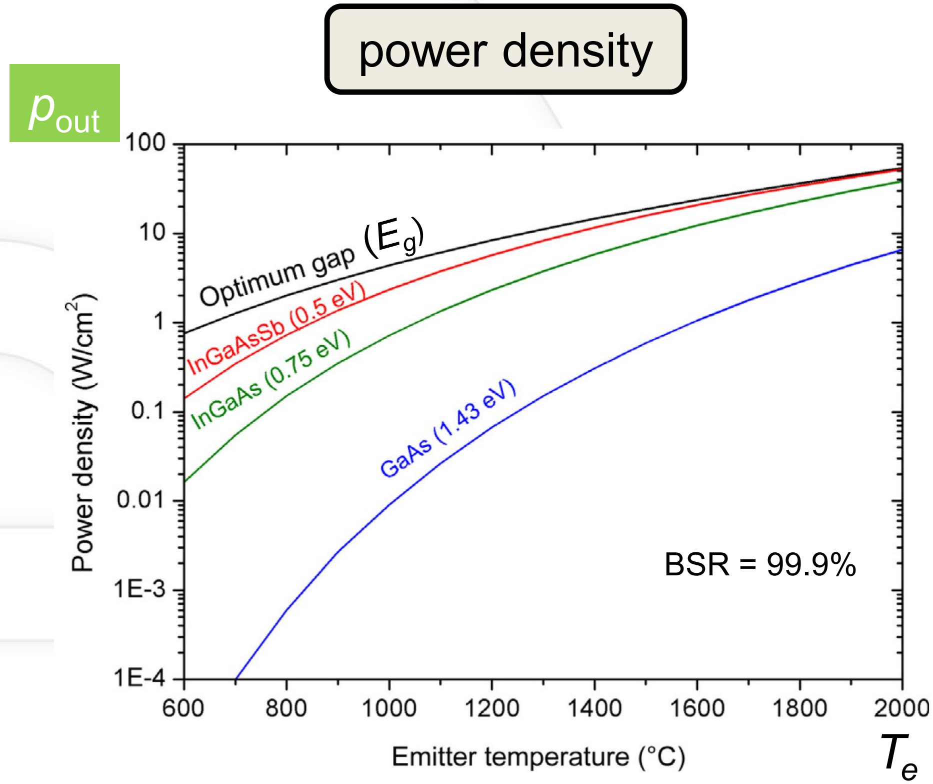

Far field

Datas & Vaillon, book chapter, 2020

Major impact of reflecting out-of-band photons

Output power density p_{out}

Resistive losses…

d = 100 nm

[Milovich et al., JPE, 2020]

PV cell surface area = 1 mm²

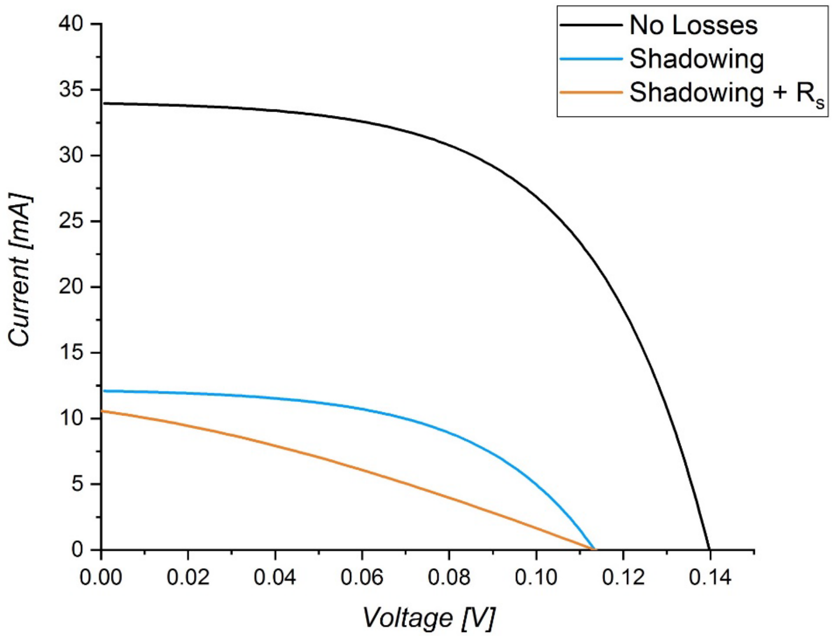

n_f = 3
w_f = 48 µm
(l = 333 µm)
P_{mpp} = 2.686 mW (without losses)
P_{mpp} = 0.365 mW (with losses)

PV cell surface area = 25 mm²

Same grid as for the 1 mm² cell

n_f = 15
w_f = 48 µm
(l = 333 µm)
P_{mpp} = 67.1 mW (without losses)
P_{mpp} = 0.00 mW (with losses)

Optimized grid for the 25 mm² cell

n_f = 6
w_f = 298 µm
(l = 833 µm)
P_{mpp} = 67.1 mW (without losses)
P_{mpp} = 1.00 mW (with losses)

Thermoelectrics vs. thermophotovoltaics

p_{out}

Near field — [Lucchesi et al., Nano Letters, 2021]

Far field — [LaPotin et al., Nature, 2022]

W / cm²

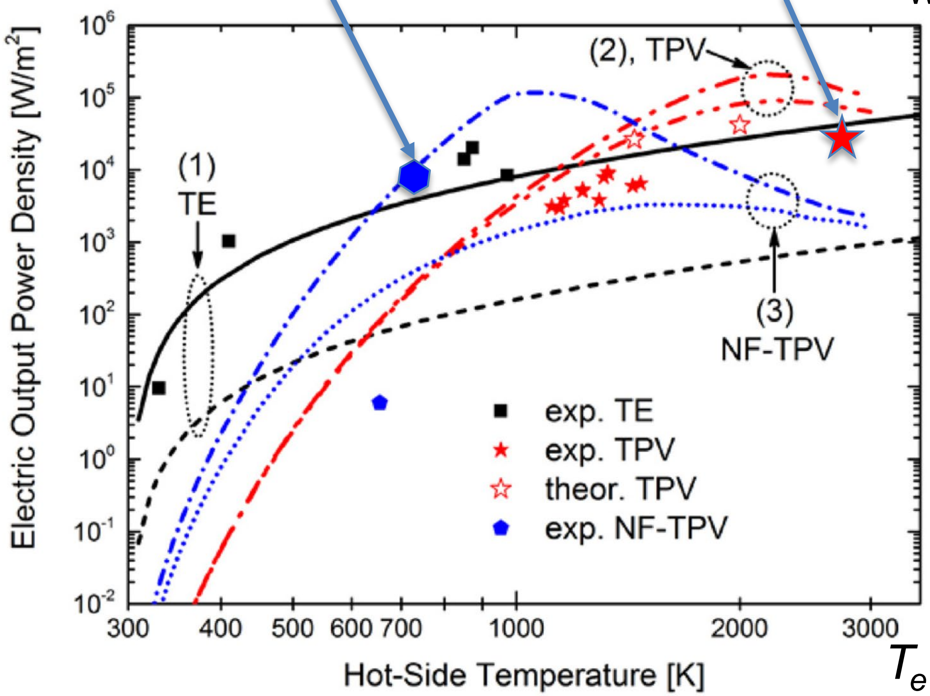

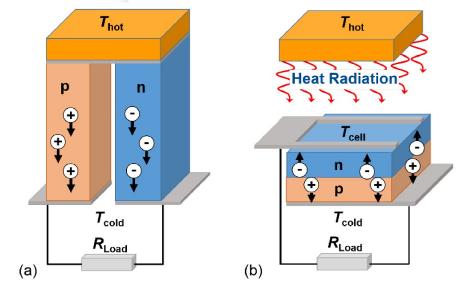

Figure 7. Electric output power density as a function of the hot-side temperature assuming a cold-side temperature of 300 K in case of direct heat radiation conversion (TPV) and a thermoelectric energy conversion (TE). Legend: **(1)**: TE conversion: **solid line**: total heat transfer coefficient $K_{cont} = 250$ W m^{-2} K^{-1}, **dashed line**: $K_c = 5$ W m^{-2} K^{-1}; **(2)**: TPV with heat transfer coefficient $K_{cont} = 500$ W m^{-2} K^{-1}, **dash-dot line**: without sub-bandgap radiation, **dash-dot-dot line**: with sub-bandgap radiation; **(3)** NF-TPV with $K_{cont} = 500$ W m^{-2} K^{-1}: **dash-dot line**: without sub-bandgap radiation, **dotted line**: with sub-bandgap radiation; **solid squares**: experimental data for TE, taken from [52–54, 57], **solid stars**: experimental data for TPV from [33, 41, 58]; **solid pentagon**: experimental data for NF-TPV, extracted from [36]; **open stars**: theoretical predictions for TPV from [41, 55].

ATTENTION — Specific assumptions in some models

[Irene Ambo Okanimba Tedah et al., JPDAP, 2019]

Thermoelectrics vs. thermophotovoltaics

Near field
Lucchesi et al., Nano Letters, 2021

Far field
LaPotin et al., Nature, 2022

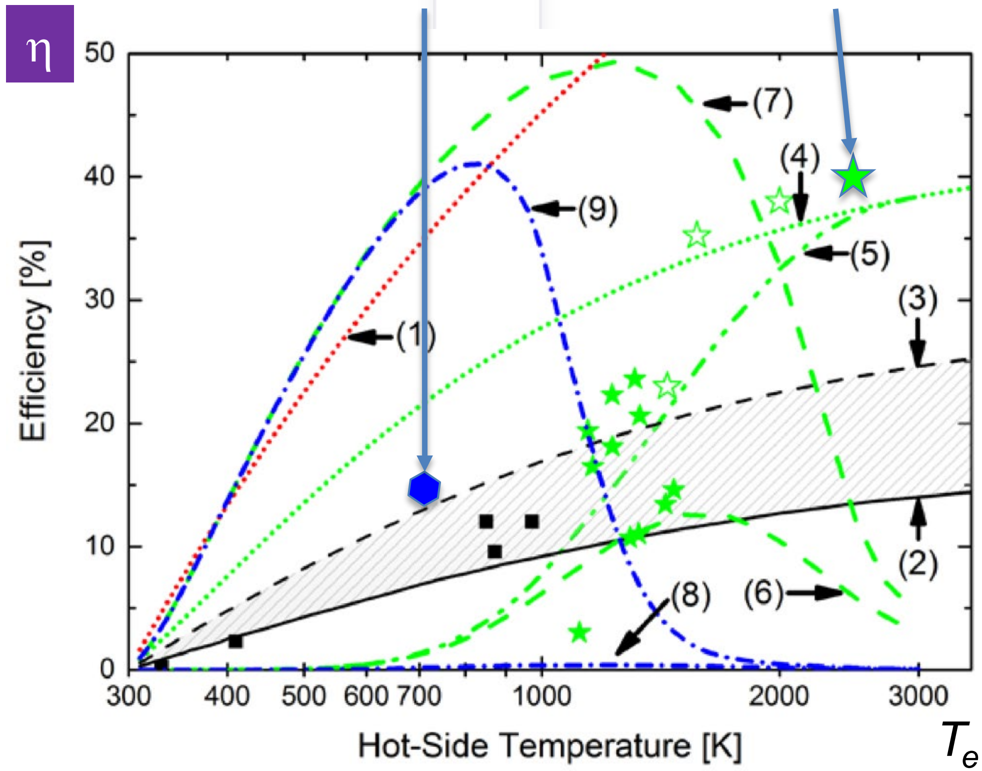

Figure 5. Different efficiency limits as a function of hot-side temperature, assuming a cold-side temperature of 300 K. **(1)**: Novikov–Curzon–Ahlborn (NCA) efficiency (equation (2)); **(2)**: TE efficiency under maximum power transfer for $ZT = 1$; **(3)**: maximum TE-efficiency for $ZT = 1$; **(4)**: conventional radiative detailed balance (RDB) limit, if non-radiative transitions would be negligible, **(5)**: RDB limit, while $E_g \geqslant 0.5$ eV in order to prevent non-radiative transitions; **(6)**: RDB –limit, taking cell heating into account by a heat transfer coefficient of $K_{cont} = 500$ W m^{-2} K^{-1}; **(7)**: RDB limit with cell heating but suppressed sub-bandgap radiation. **(8)**: RDB limit for NF-TPV with cell heating and sub-bandgap radiation, **(9)**: RDB limit for NF-TPV with cell heating but without sub-bandgap emission. For NF-TPV a 40-fold enhanced black body radiation was assumed. Data from literature are added for comparison. These are: **solid squares**: experimental data of TEGs, taken from [52–54, 57], **solid stars**: experimental data of TPV cells, taken from [33, 41, 58], **open stars**: simulated TPV cells with photonic engineered/spectral shaped emitter materials [41, 42, 55].

ATTENTION Specific assumptions in some models

Irene Ambo Okanimba Tedah et al., JPDAP, 2019

Ultrathin PV cells → TPV cells?

?

↓ material consumption using thin film cells

Ultrathin solar cells

Massiot et al., Nature Energy, 2014

GaAs

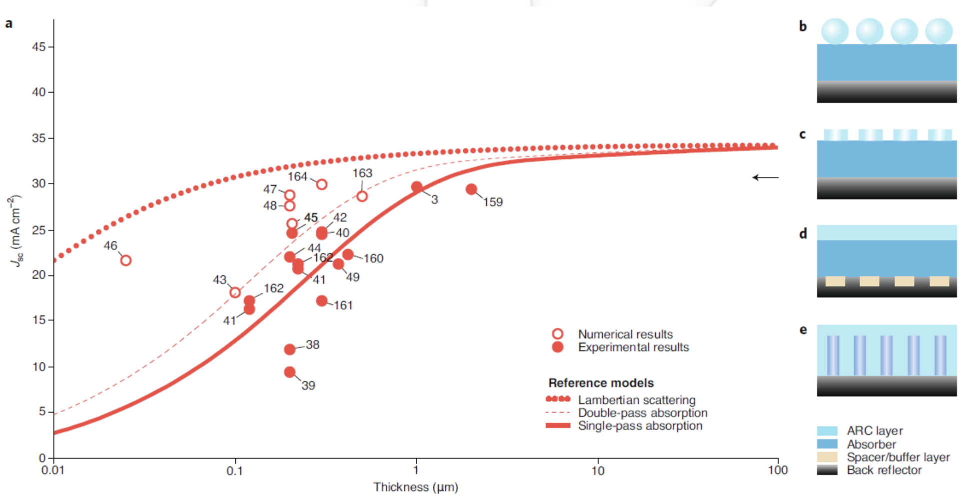

light trapping schemes

b, **c**: front dielectric nanostructure arrays
d: nanostructured back mirror
e: nanowire arrays

Application to TPV?

Theo.

Near field

less nonradiative recombination

η

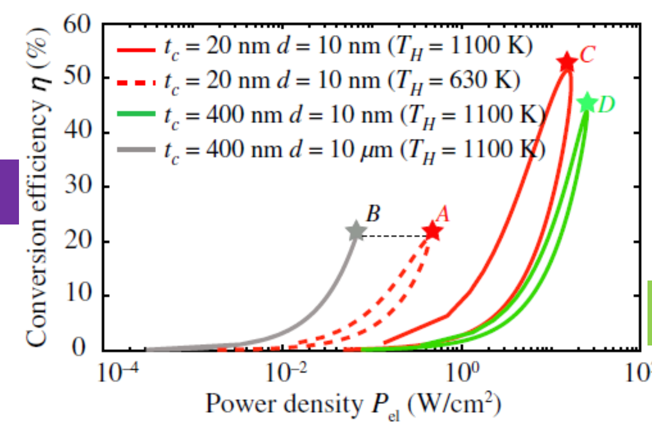

p_{out}

Papadakis et al., Phys. Rev. Applied, 2021

+ resistive losses?

Modelling considering various nanostructures and all losses